NSTX-U Seminar, Princeton, November 14th, 2016

Inter-ELM pedestal evolution in ASDEX Upgrade: Magnetic activity correlated with the recovery of the edge profiles

F. M. Laggner[1]

E. Wolfrum[2], M. Cavedon[2,3], M. G. Dunne[2], F. Mink[2,3], G. Birkenmeier[2,3],
R. Fischer[2], E. Viezzer[2], M. Willensdorfer[2], F. Aumayr[1],
the ASDEX Upgrade Team[2] and the EUROfusion MST1 Team

[1]Institute of Applied Physics, TU Wien, Fusion@ÖAW, Wiedner Hauptstr. 8-10, 1040 Vienna, Austria
[2]Max-Planck-Institut für Plasmaphysik, Boltzmannstr. 2, 85748 Garching, Germany
[3]Physik-Department E28, Technische Universität München, James-Franck-Str.1, 85748 Garching, Germany

FRIEDRICH SCHIEDEL STIFTUNG FÜR ENERGIETECHNIK WIEN

F. M. Laggner is a fellow of the Friedrich Schiedel Foundation for Energy Technology

This work has been carried out within the framework of the EUROfusion Consortium and has received funding from the Euratom research and training programme 2014-2018 under grant agreement No 633053. The views and opinions expressed herein do not necessarily reflect those of the European Commission.

Outline

- Introduction to pedestal stability
- Pedestal recovery and onset of magnetic fluctuations
  - Localization, poloidal and toroidal mode structure
- Comparison of the pedestal recovery for different main ion species
  - Similar sequence of recovery phases in different species
- Connecting the evolution of the outer divertor to the pedestal recovery
  - High recycling regime connected to density evolution
- Summary & conclusions

Pedestal stability

- Peeling-ballooning P-B theory:

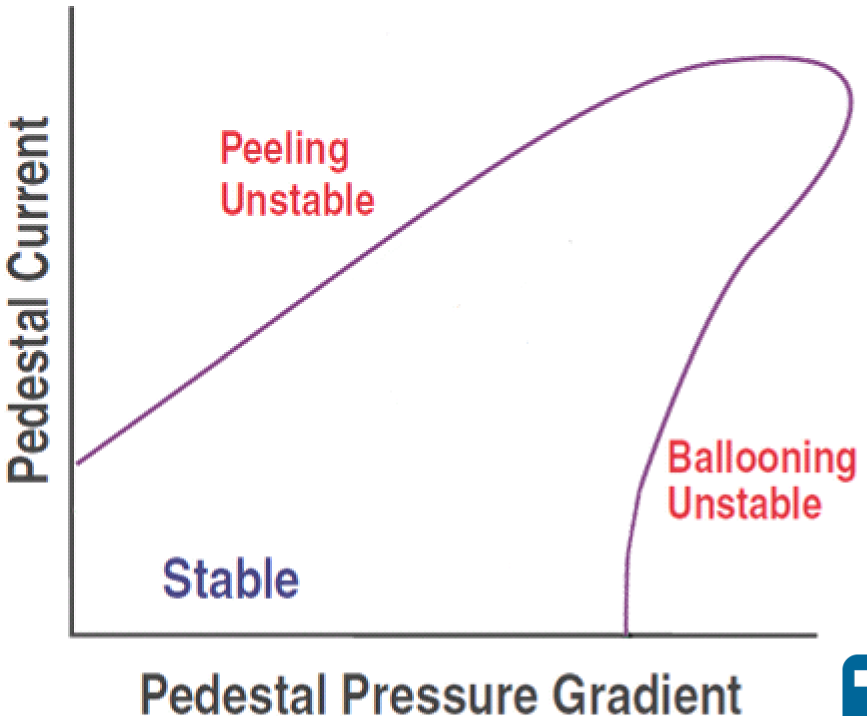

[P. B. Snyder et al., POP 2009]

Pedestal stability

- Peeling-ballooning P-B theory:
  - Peeling Mode
    - ➢ Current driven instability

[G. Huysmans, PPCF 2005]

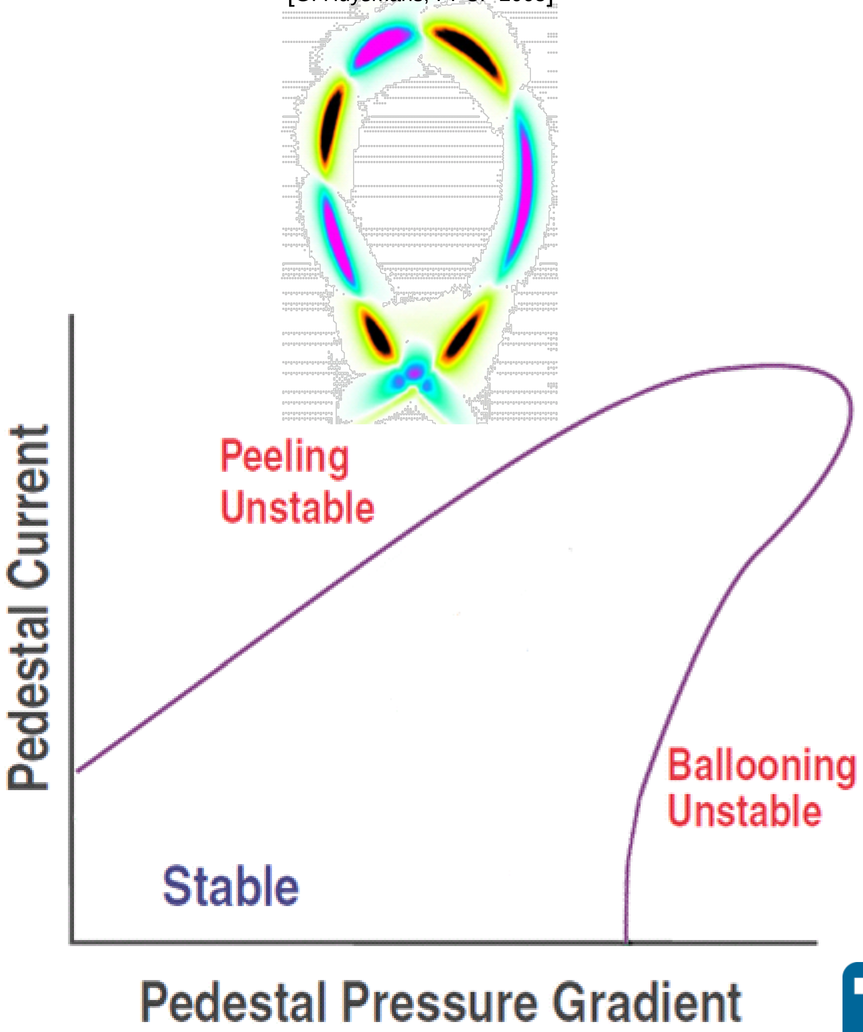

[P. B. Snyder et al., POP 2009]

Pedestal stability

- Peeling-ballooning P-B theory:
  - Peeling Mode
    - ➢ Current driven instability
  - Ballooning Mode
    - ➢ Pressure driven instability

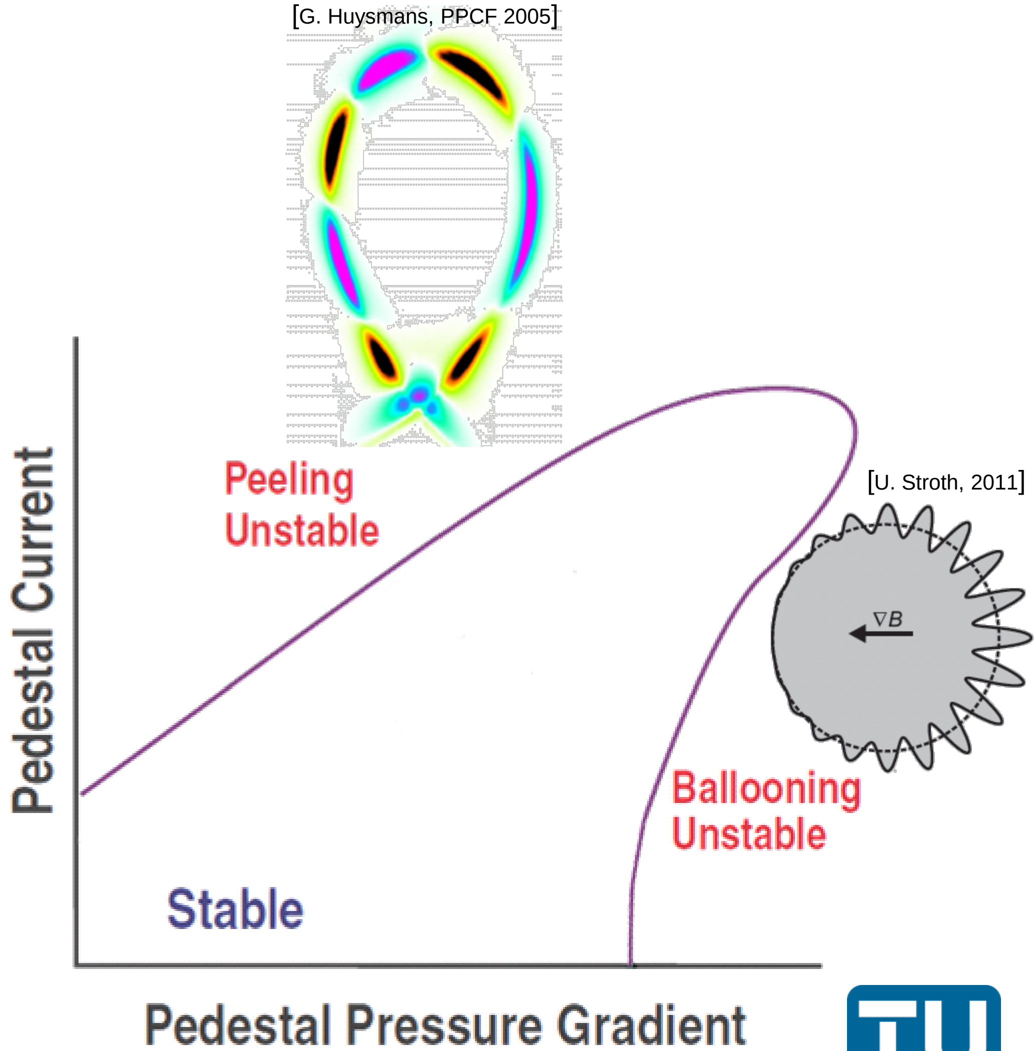

[P. B. Snyder et al., POP 2009]

Pedestal stability

- Peeling-ballooning P-B theory:
  - Peeling Mode
    - ➢ Current driven instability
  - Ballooning Mode
    - ➢ Pressure driven instability

- P-B gives a ‘hard’ limit for the edge pressure

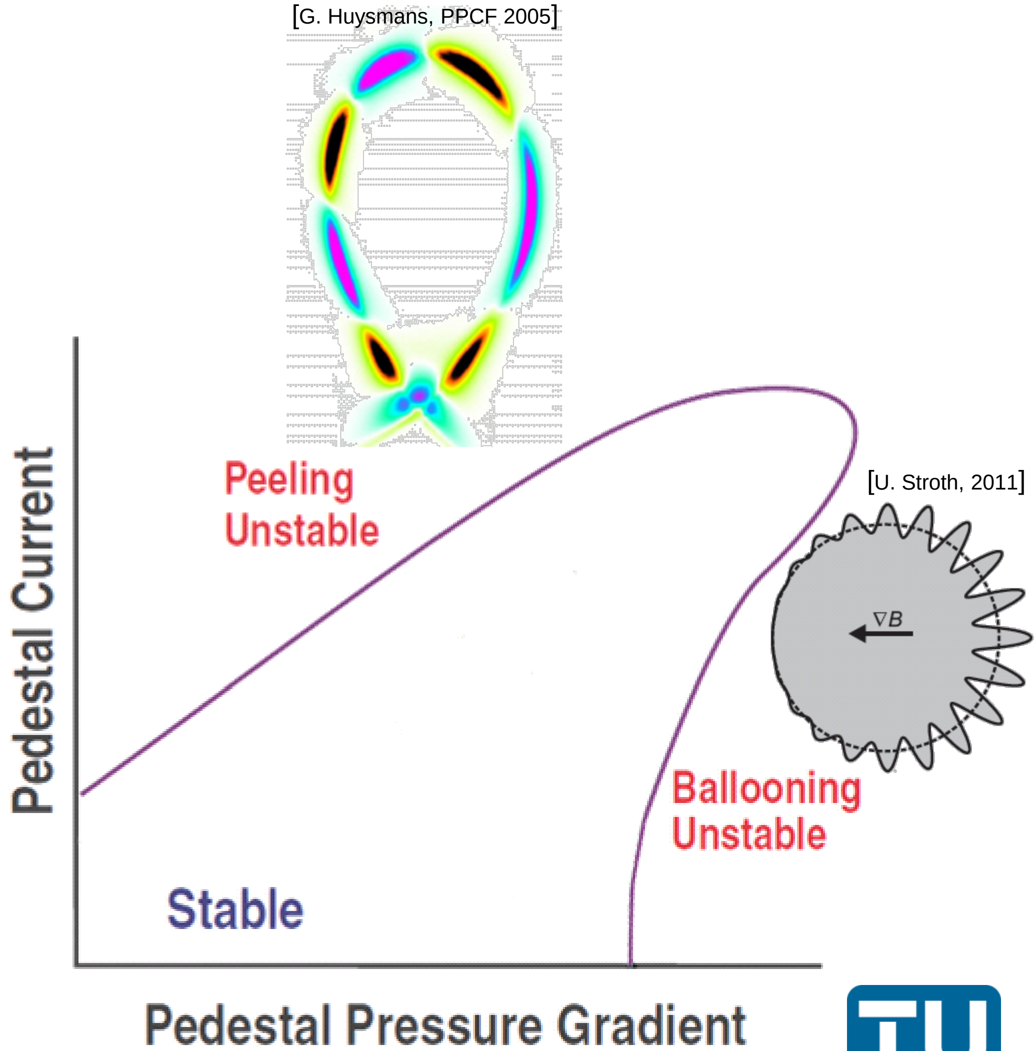

[P. B. Snyder et al., POP 2009]

Pedestal evolution – ELM cycle

- Model for type-I ELM cycle

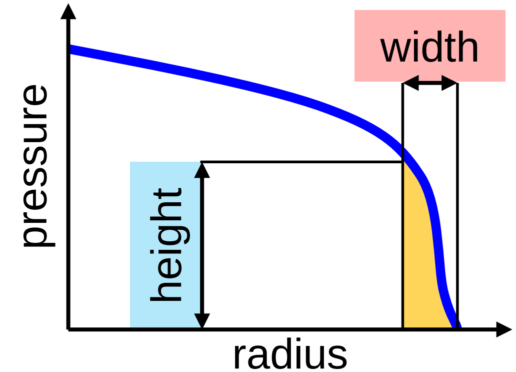

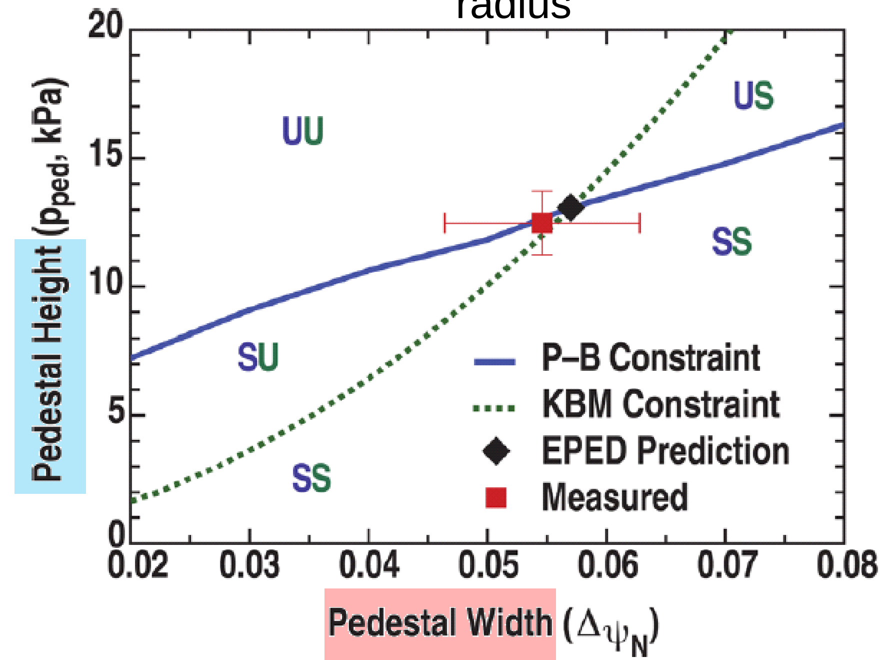

[P. B. Snyder et al., POP 2012]

Pedestal evolution – ELM cycle

- Model for type-I ELM cycle
  - (1) Pedestal height and width increase till kinetic ballooning mode (KBM) boundary ('soft limit') is reached

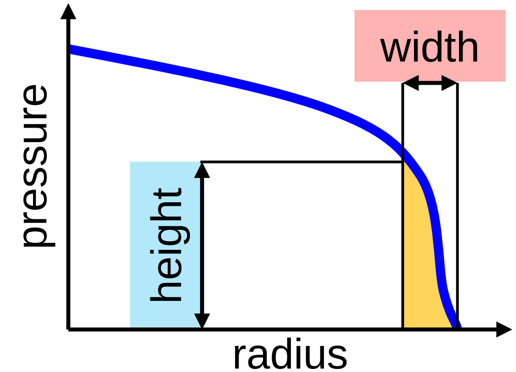

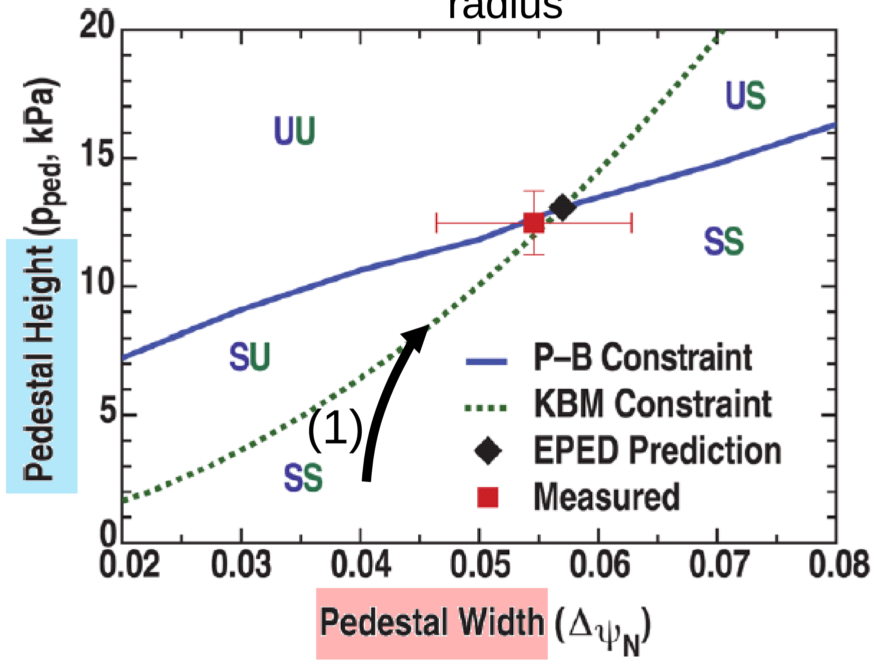

[P. B. Snyder et al., POP 2012]

Pedestal evolution – ELM cycle

- Model for type-I ELM cycle
  - (1) Pedestal height and width increase till kinetic ballooning mode (KBM) boundary ('soft limit') is reached
  - (2) Pedestal gradient is clamped and height and width evolve along the KBM limit

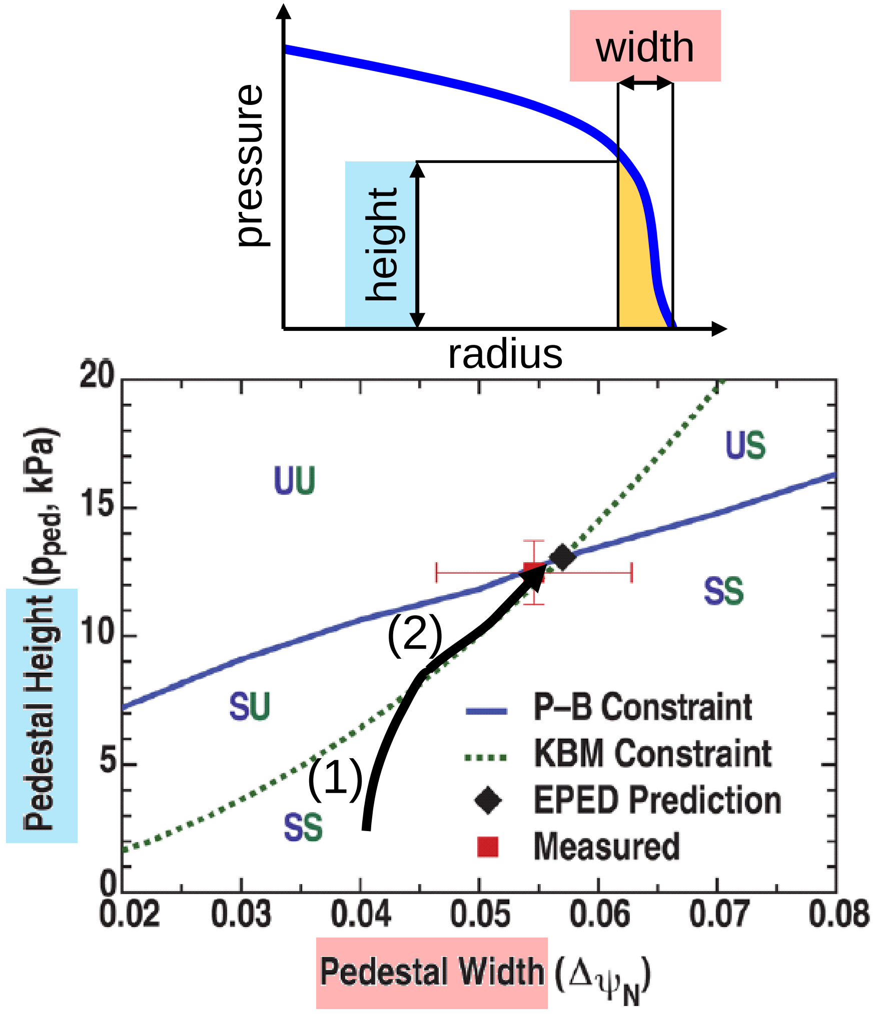

[P. B. Snyder et al., POP 2012]

Pedestal evolution – ELM cycle

- Model for type-I ELM cycle
  - (1) Pedestal height and width increase till kinetic ballooning mode (KBM) boundary ('soft limit') is reached
  - (2) Pedestal gradient is clamped and height and width evolve along the KBM limit
  - (3) ELM crash when P-B ('hard') limit is reached

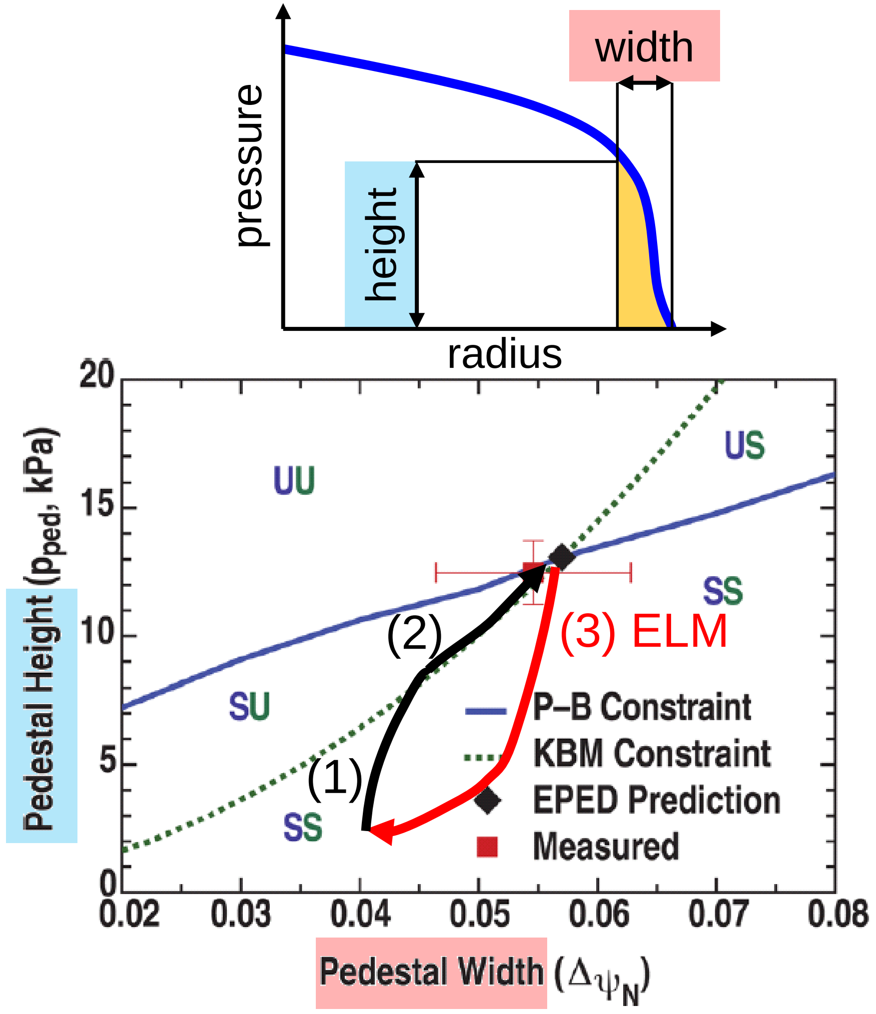

[P. B. Snyder et al., POP 2012]

Pedestal evolution – ELM cycle

- Model for type-I ELM cycle
  - (1) Pedestal height and width increase till kinetic ballooning mode (KBM) boundary ('soft limit') is reached
  - (2) Pedestal gradient is clamped and height and width evolve along the KBM limit
  - (3) ELM crash when P-B ('hard') limit is reached

- Limitation of pedestal evolution ('soft limit') observed in several experiments

[A. Burckhart et al., PPCF 2010]

[D. Dickinson et al., PRL 2012]

[A. Diallo et al., PRL 2014]

[A. Diallo et al., POP 2015]

[X. Gao et al., NF 2015]

[X. Zhong et al., PPCF 2016]

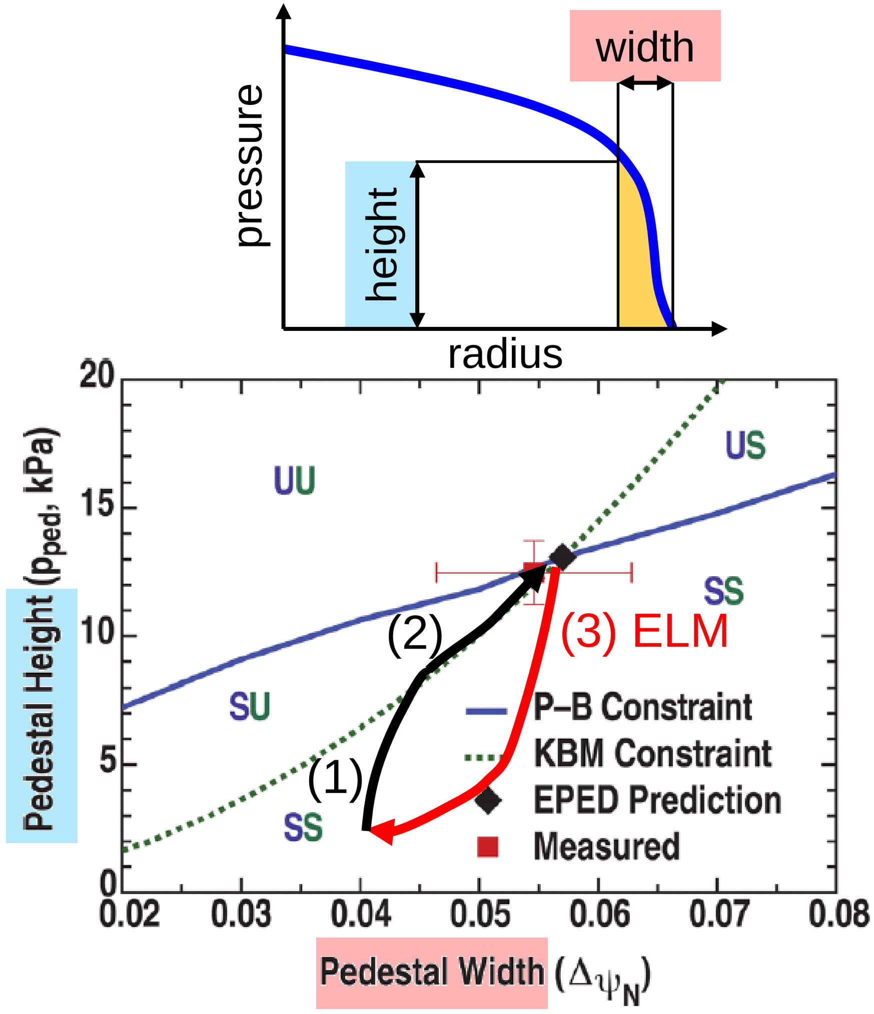

[P. B. Snyder et al., POP 2012]

Previous observations at AUG…

ASDEX Upgrade

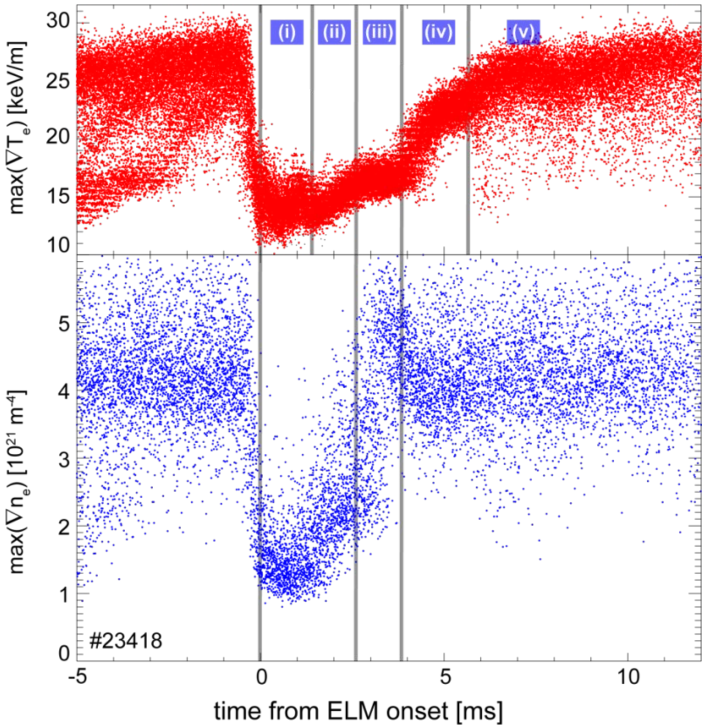

[A. Burckhart et al., PPCF 2010]

ELM synchronization

- ELMs are quasi-periodic events
  - ➢ Increase amount of data by averaging over several ‘equal’ ELMs

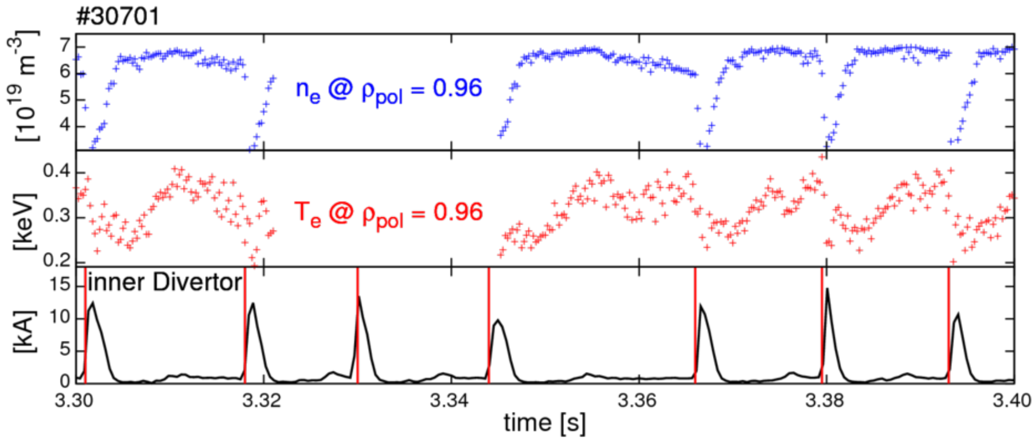

ELM synchronization

- ELMs are quasi-periodic events
  - ➢ Increase amount of data by averaging over several ‘equal’ ELMs
- Procedure:
  - Determination of individual ELM onset

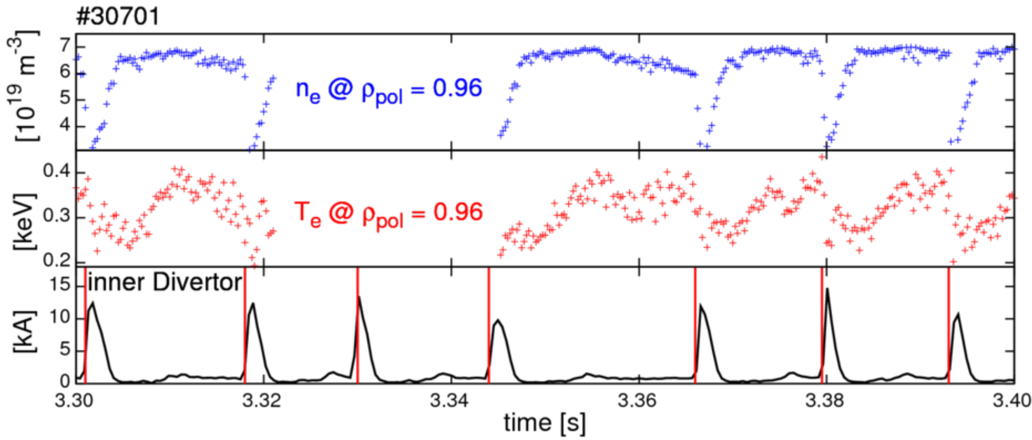

ELM synchronization

- ELMs are quasi-periodic events
  - ➢ Increase amount of data by averaging over several ‘equal’ ELMs

- Procedure:
  - Determination of individual ELM onset
  - Collapse time base relative to ELM onset

- Statistically significant effects are conserved

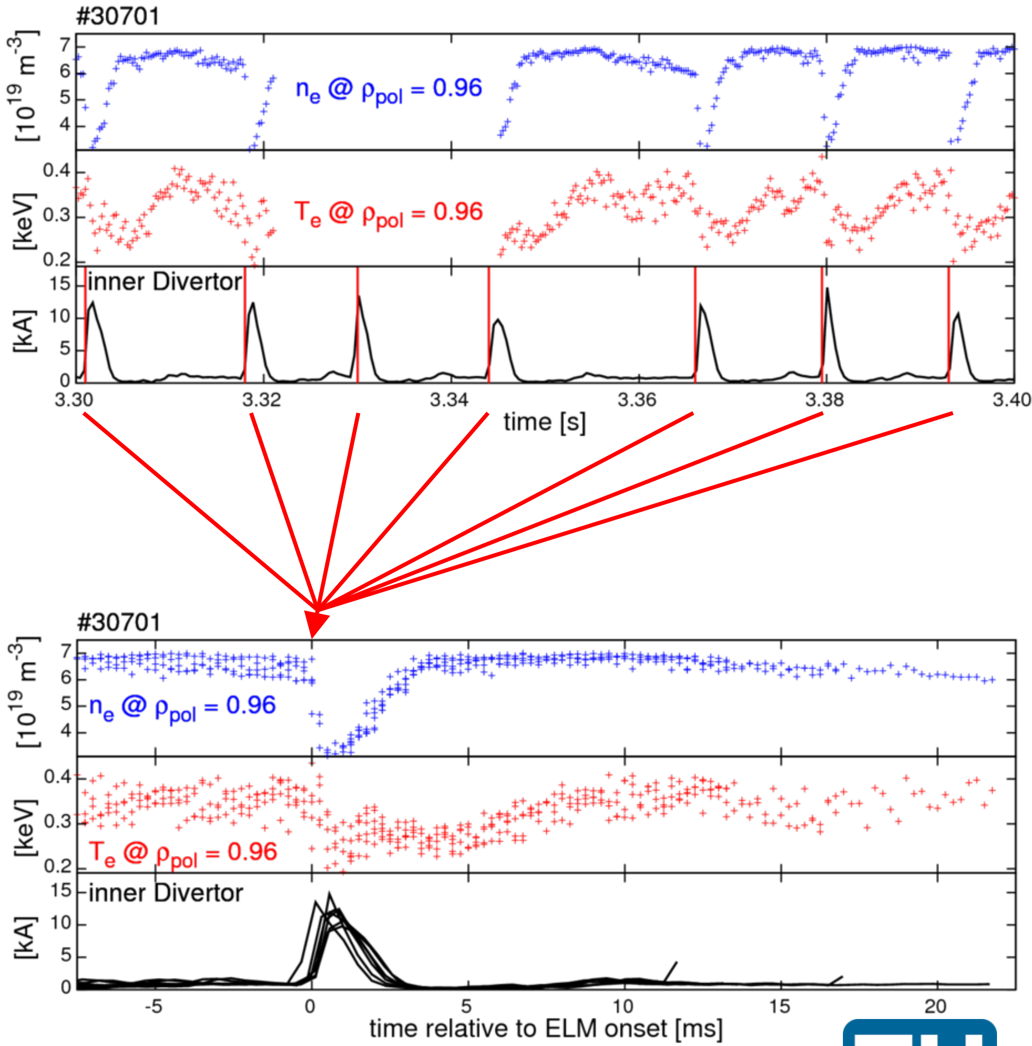

Previous observations at AUG…

- n_e and T_e recover on different timescales
  - First, max(∇ n_e) recovery, then max(∇T_e)
- max(∇T_e) established several milliseconds before onset of ELM crash

ASDEX Upgrade

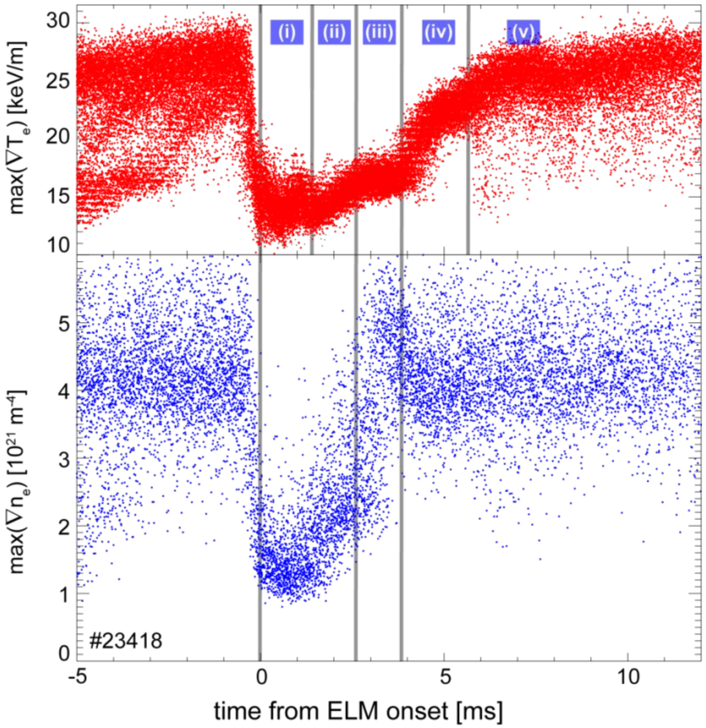

[A. Burckhart et al., PPCF 2010]

...in the US...

- Magnetic fluctuations when pedestal top T_e is recovered

DIII-D

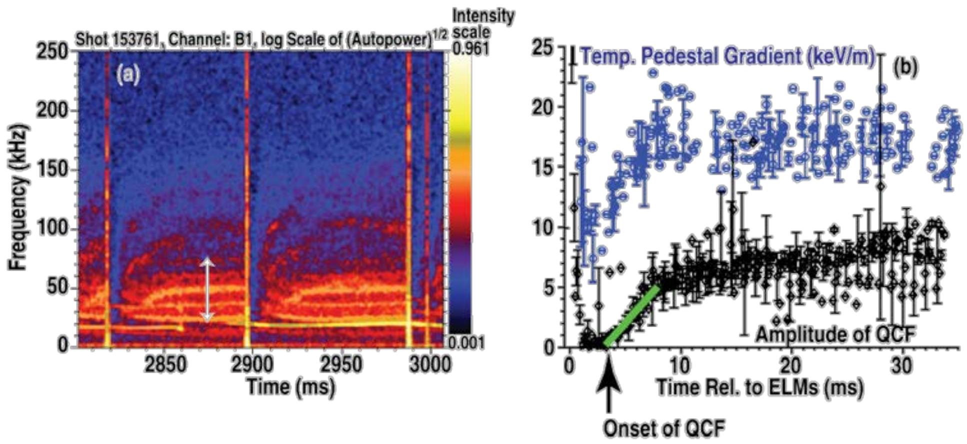

[A. Diallo et al., POP 2015]

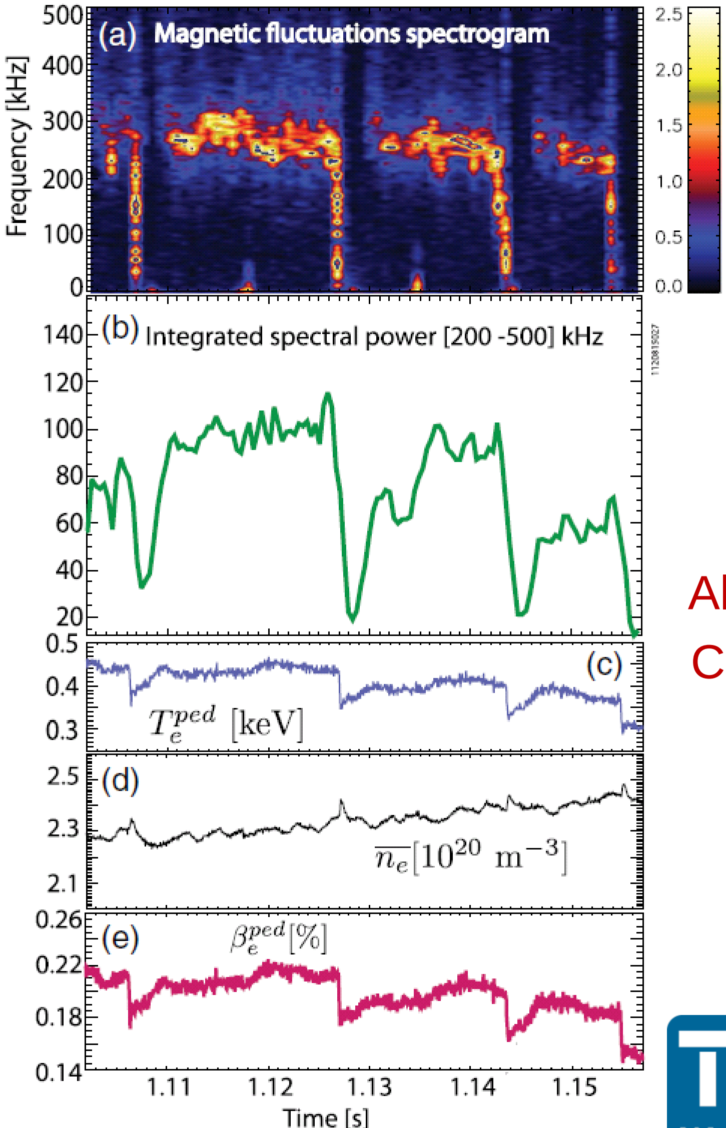

Alcator C-Mod

[A. Diallo et al., PRL 2014]

...and in Asia

HL-2A

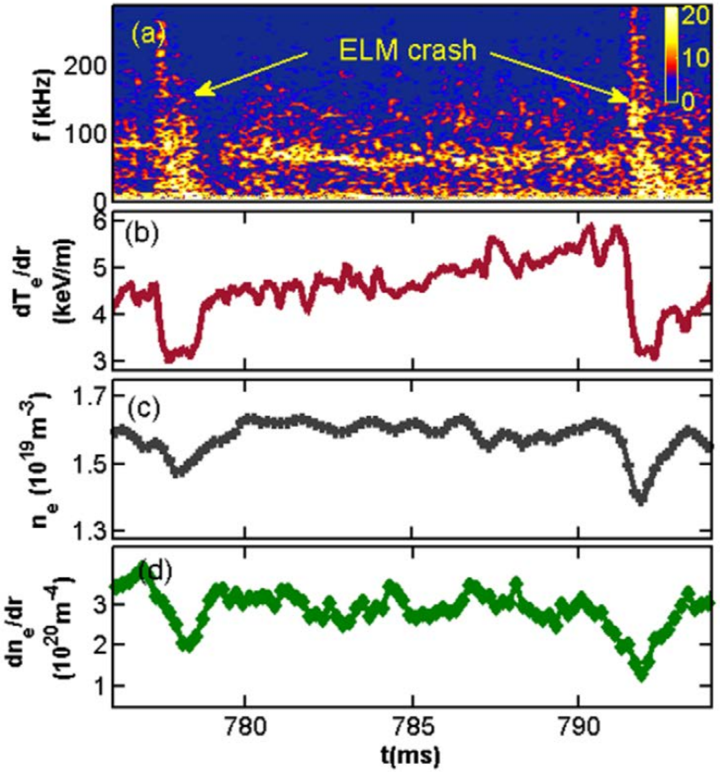

[W. L. Zhong et al., PPCF 2016]

EAST

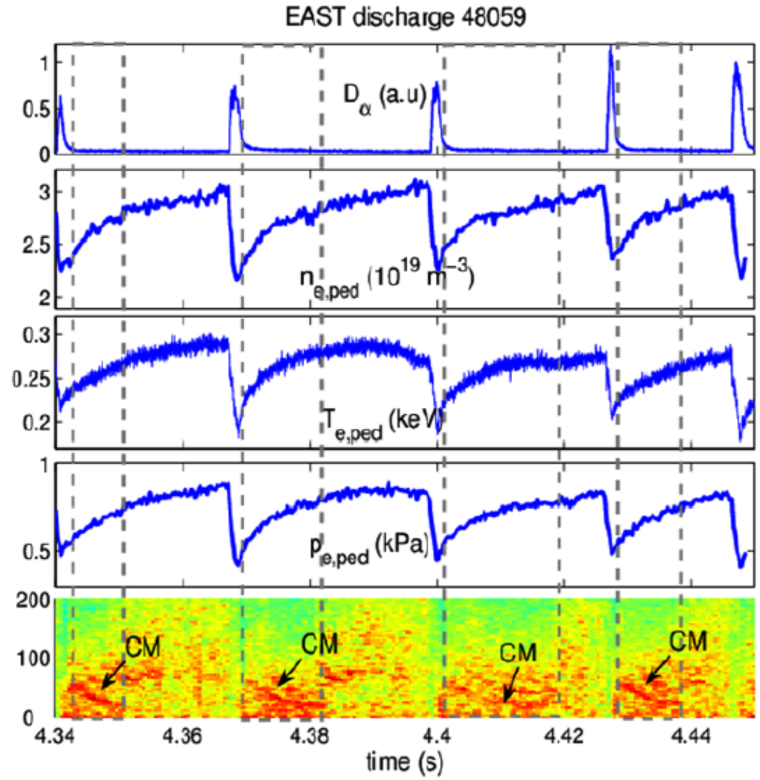

[X. Gao et al., NF 2015]

...and in Asia

HL-2A

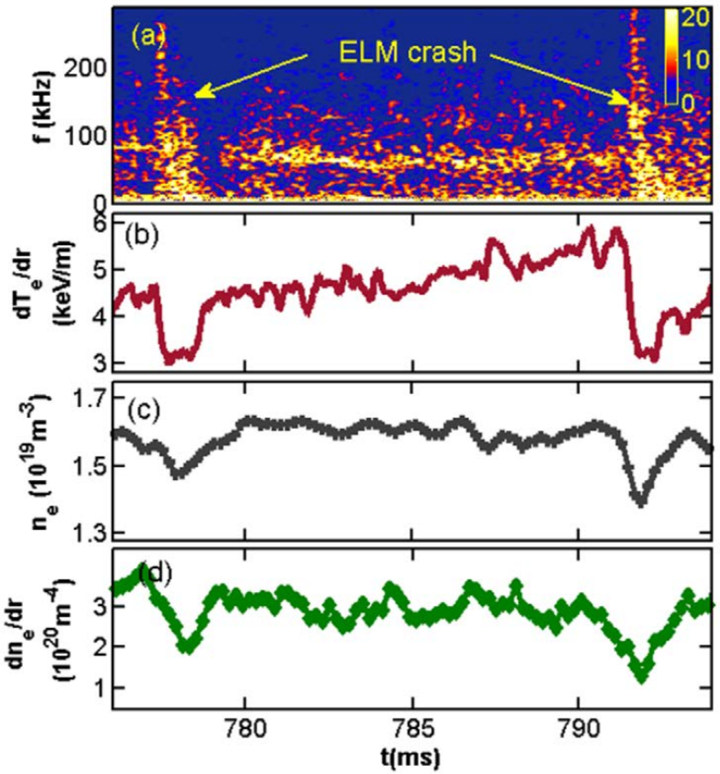

[W. L. Zhong et al., PPCF 2016]

EAST

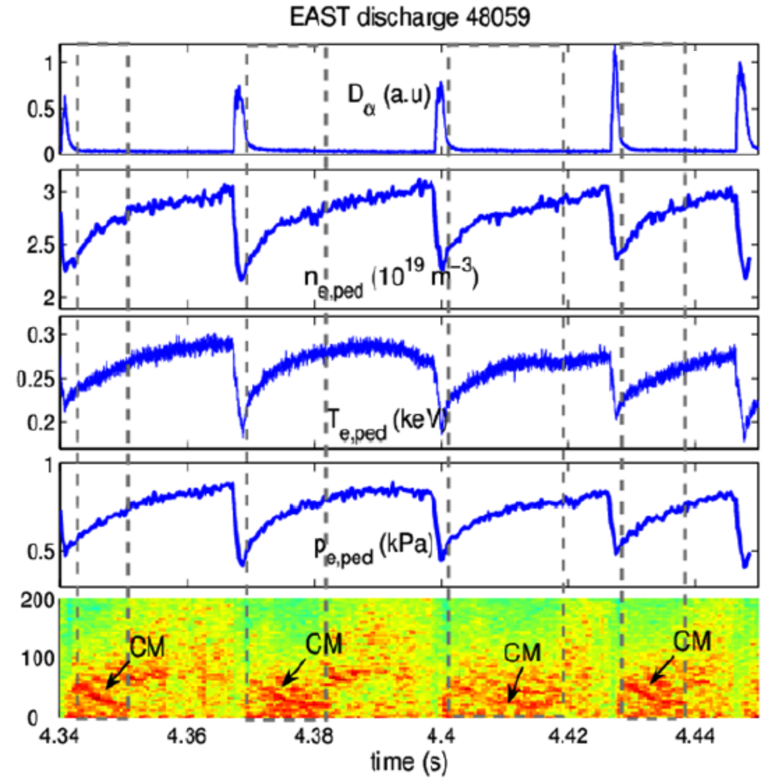

[X. Gao et al., NF 2015]

→ Can we get deeper insight in the underlying instabilities?

Profile measurements at AUG

- Electron density (n_e) and electron temperature (T_e)
  - Utilisation of integrated data analysis (IDA)
    [R. Fischer et al., FST 2010]
    - ➢ Li-Beam and interferometry for n_e
    - ➢ ECE for T_e
      - – ECFM to model ECE propagation in the optically thin plasma
        [S.K. Rathgeber et al., PPCF 2013]
  - Profiles evaluated 250 μs time resolution

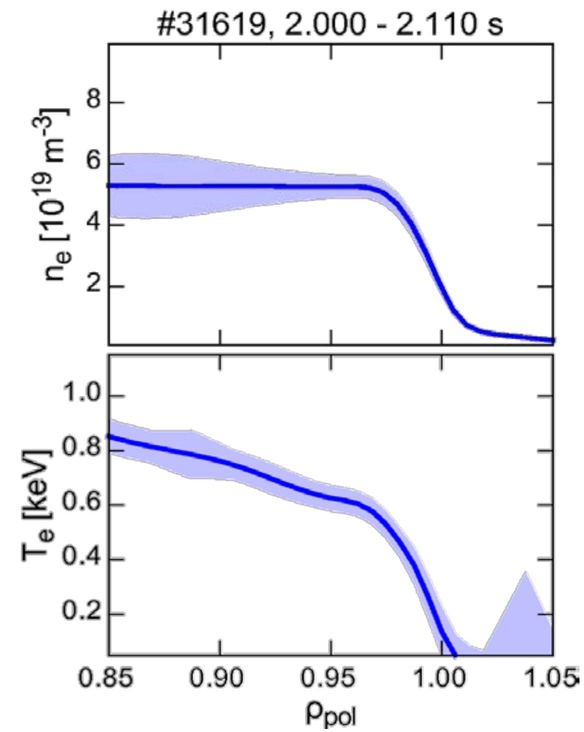

Outline

- Introduction to pedestal stability
- Pedestal recovery and onset of magnetic fluctuations
  - Localization, poloidal and toroidal mode structure
- Comparison of the pedestal recovery for different main ion species
  - Similar sequence of recovery phases in different species
- Connecting the evolution of the outer divertor to the pedestal recovery
  - High recycling regime connected to density evolution
- Summary & conclusions

Two discharges having similar p_e

- High (#30701) and low (#30721) pedestal top electron collisionality $\nu^*_{e,ped}$
- Motivation for comparison:
  - Pressure (gradient) driven instabilities should not change their behavior

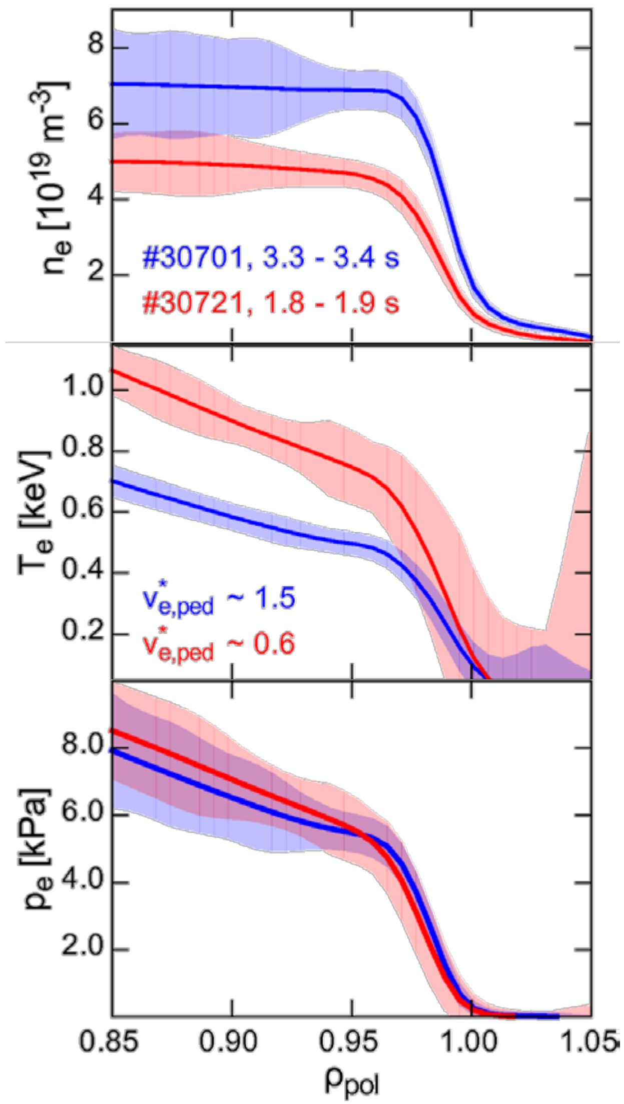

Two discharges having similar p_e

- High (#30701) and low (#30721) pedestal top electron collisionality $\nu^*_{e,ped}$
- Motivation for comparison:
  - Pressure (gradient) driven instabilities should not change their behavior
- In both discharges gradients are clamped before the ELM onset (‘soft limit’)

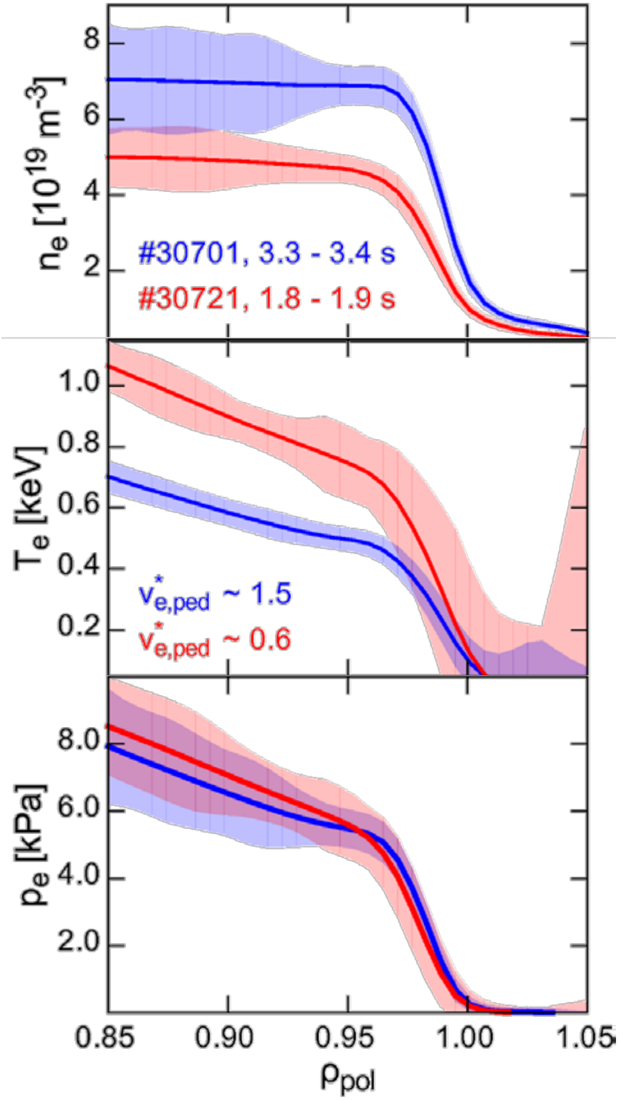

Similar recovery of n_e and T_e

High $\nu^*_{e,ped}$ (#30701) case

- First $n_{e,ped}$ recovery (Δt_{n_e}), then $T_{e,ped}$ (Δt_{T_e})
  [A. Burckhart et al., PPCF 2010]
- Fluctuations start after Δt_{T_e}

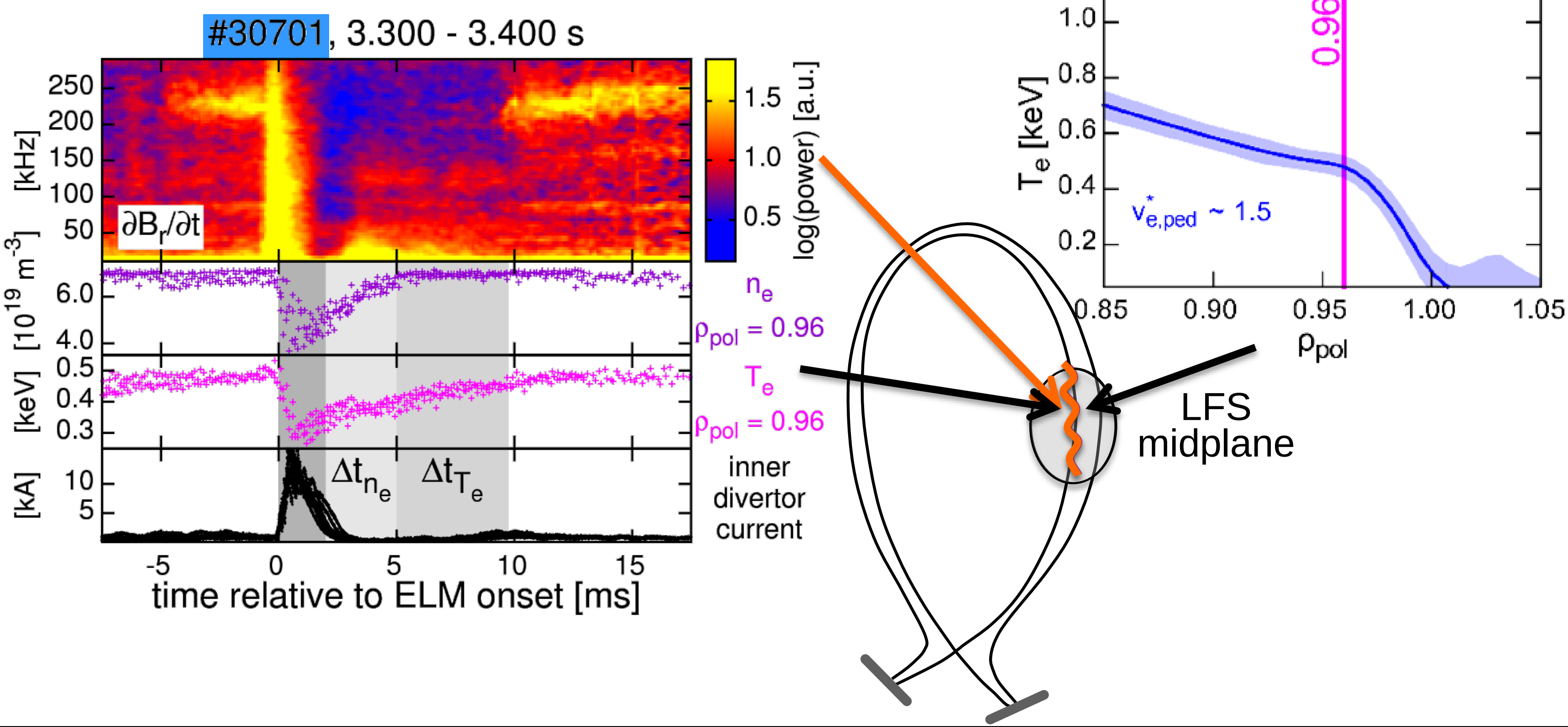

Similar recovery of n_e and T_e

High $\nu^*_{e,ped}$ (#30701) case

- First $n_{e,ped}$ recovery (Δt_{n_e}), then $T_{e,ped}$ (Δt_{T_e})
  [A. Burckhart et al., PPCF 2010]
- Fluctuations start after Δt_{T_e}

Low $\nu^*_{e,ped}$ (#30721) case

- Similar phases
- High frequency fluctuations also start after Δt_{T_e}

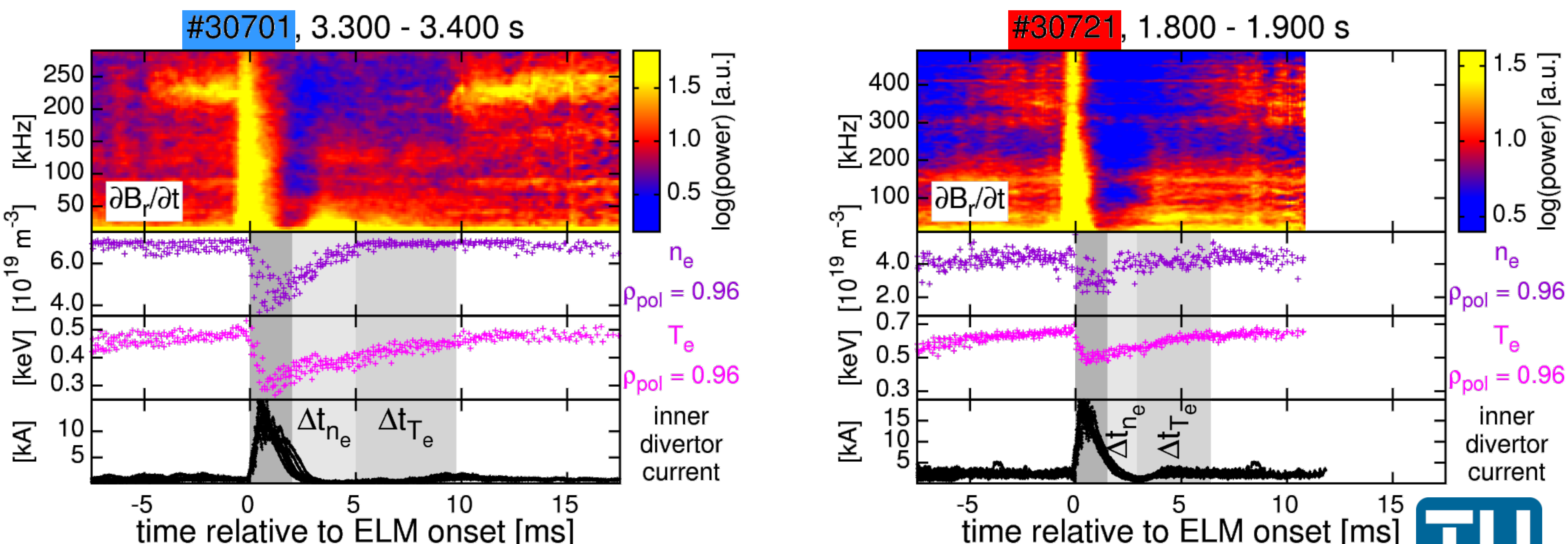

→ Fluctuations correlated to the recovery of $n_{e,ped}$ & $T_{e,ped}/p_{e,ped}$

∇n_e and ∇T_e clamped before ELM

High $\nu^*_{e,ped}$ (#30701) case

- max(∇n_e) and max(∇T_e) evolve till high frequency fluctuation onset

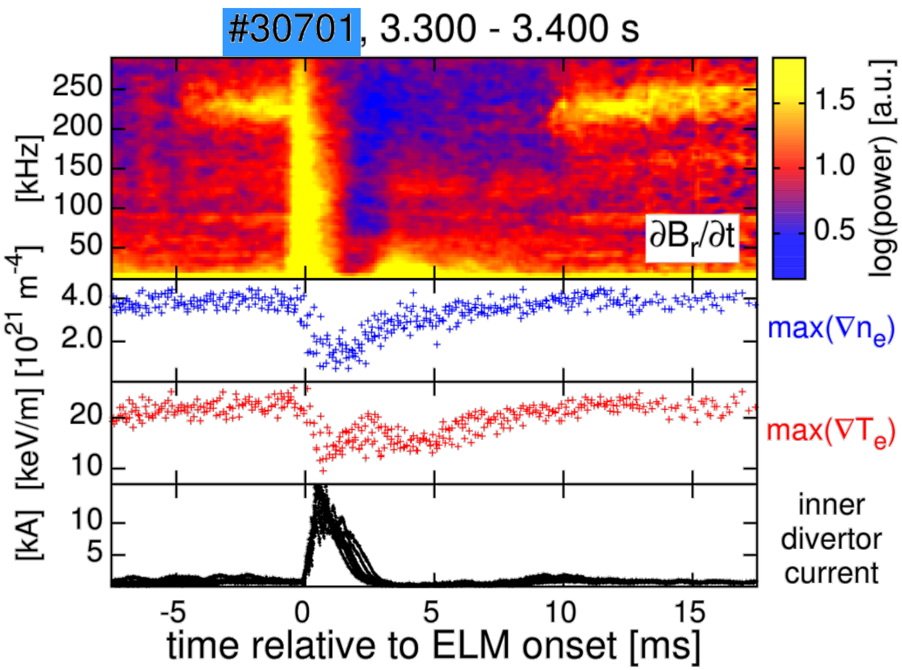

∇n_e and ∇ T_e clamped before ELM

High $\nu^*_{e,ped}$ (#30701) case

- max(∇n_e) and max(∇T_e) evolve till high frequency fluctuation onset

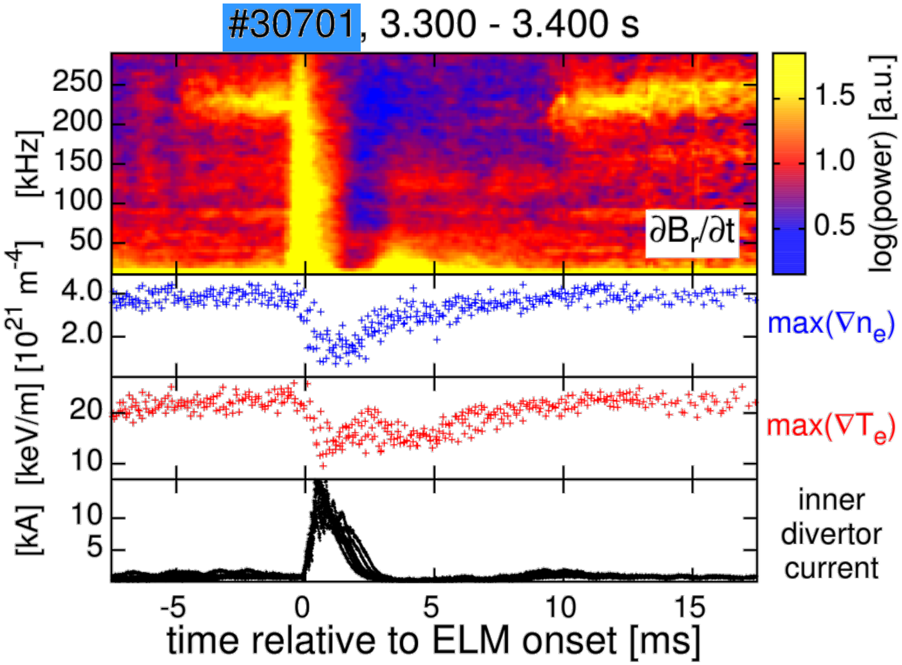

Low $\nu^*_{e,ped}$ (#30721) case

- Gradients are also clamped after onset of fluctuations
- Fluctuations have much higher frequency

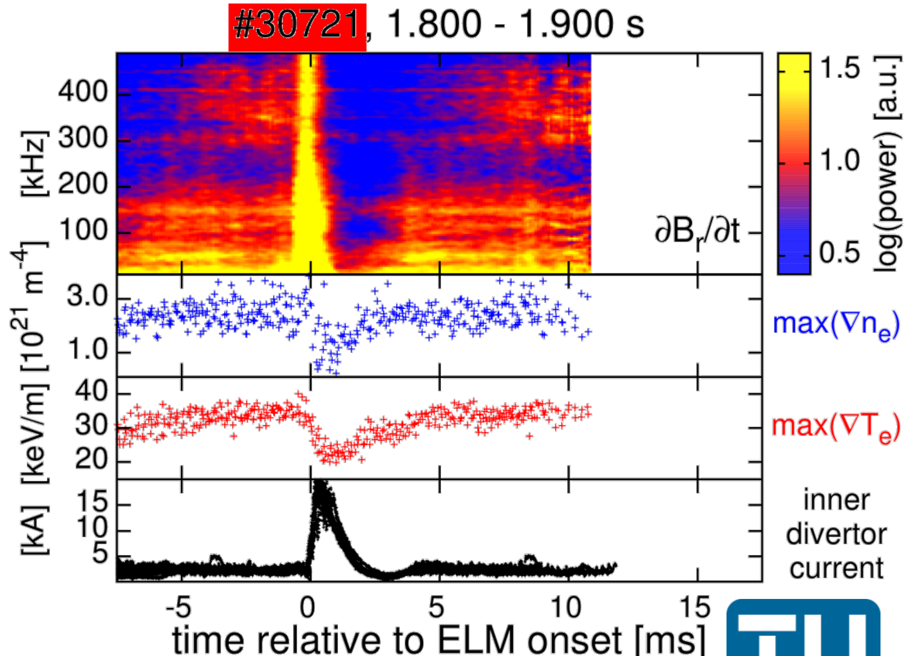

→ What determines the detected fluctuation frequency?

Mode propagation – E×B velocity

- H-mode → strong E×B background velocity at the edge

- In the steep gradient region E_r is well described by estimation $\nabla p_i/en_i$

  [E. Viezzer et al., NF 2014]

- E_r and $\nabla p_e/en_e$ agree within their errors in the analyzed cases
  - Estimation of background velocity by $\nabla p_e/en_e$ valid

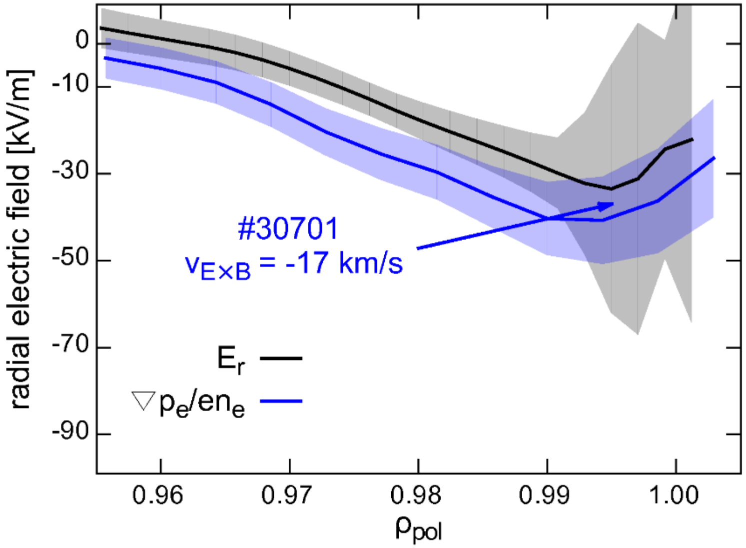

Mode propagation – E×B velocity

- H-mode → strong E×B background velocity at the edge
- In the steep gradient region E_r is well described by estimation $\nabla p_i/en_i$

  [E. Viezzer et al., NF 2014]

- E_r and $\nabla p_e/en_e$ agree within their errors in the analyzed cases
  - ➢ Estimation of background velocity by $\nabla p_e/en_e$ valid

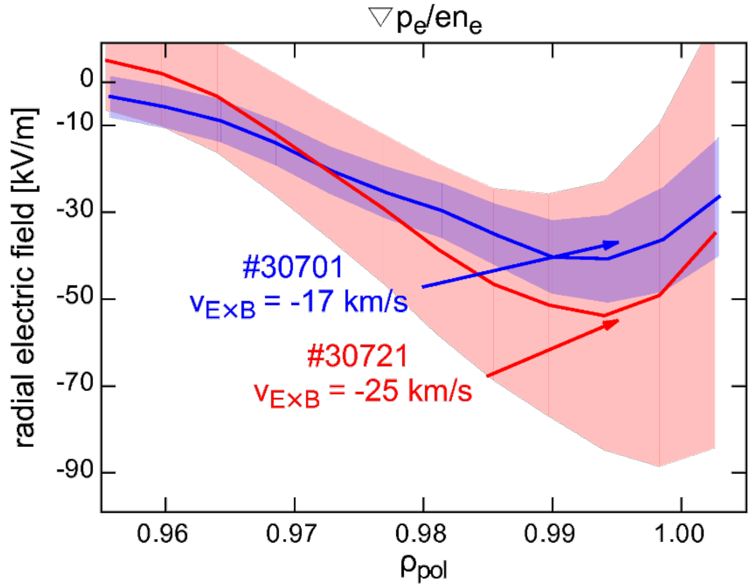

Mode propagation – E×B velocity

- 11 discharge intervals:
  - Selected to span wide range of $\nabla p_e/en_e$
  - Clear magnetic fluctuations (onset correlated to $T_{e,ped}$ recovery)

- Detected fluctuation frequency increases with $\nabla p_e/en_e$ at position of $\max(\nabla p_e)$

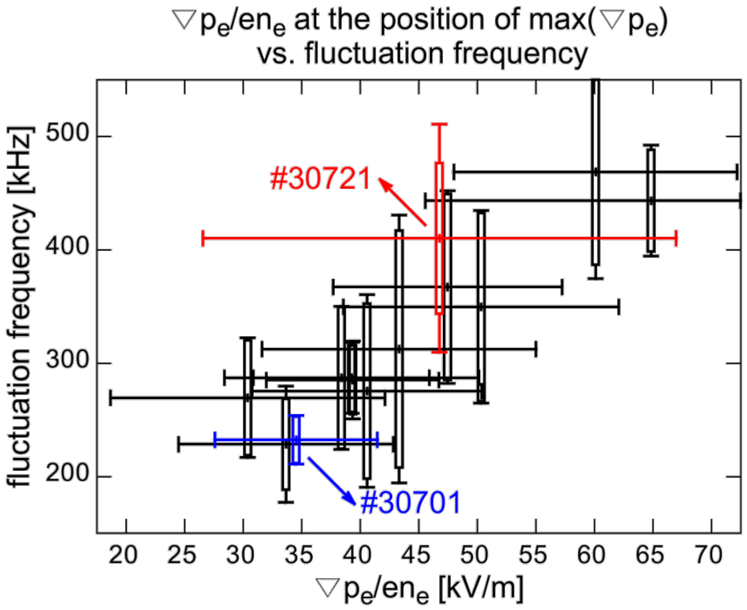

→ Mode is located in the steep gradient region

Toroidal mode structure

- Fit of n using the discharge intervals with different $\nabla p_e/en_e$

- Fit of toroidal mode number:
  - $n \sim U_{tor} \cdot f_{magn} / (v_{\nabla p_e/en_e} \cdot q \cdot U_{tor}/U_{pol} + v_{tor})$

- Fitted n ~ -11
  - Negative n
    - ➢ Counter-current or propagation in electron diamagnetic direction

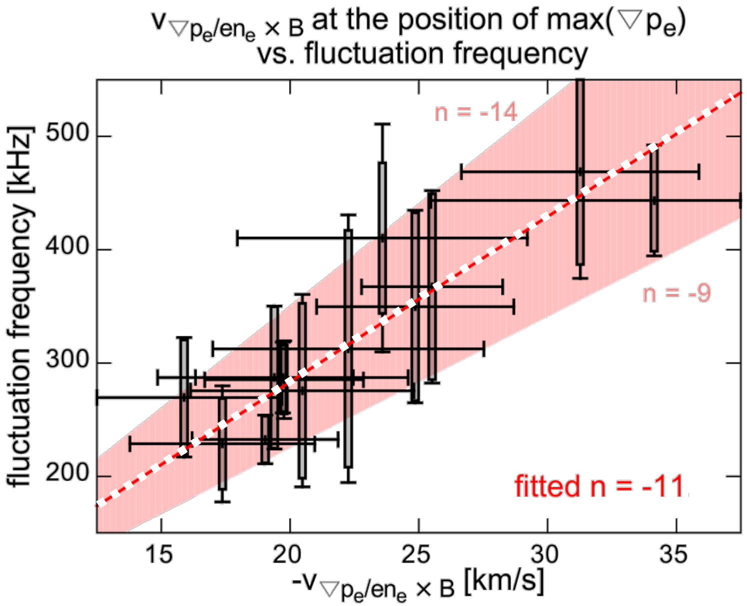

Mode number analysis

- Transfer functions of B_r coils are required

  [L. Horvath et al., PPCF 2015]

  - Especially for high toroidal mode numbers n and at high fluctuation frequencies

Top down view on AUG

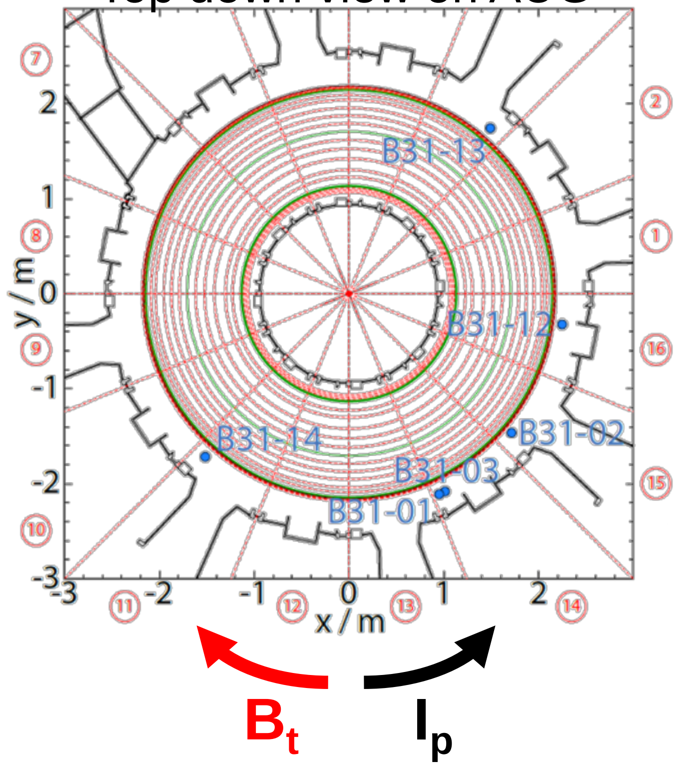

Mode number analysis

- Transfer functions of B_r coils are required

  [L. Horvath et al., PPCF 2015]

  - Especially for high toroidal mode numbers n and at high fluctuation frequencies

•Negative n:

- ➢ Counter-current propagation or propagation in electron diamagnetic direction

Top down view on AUG

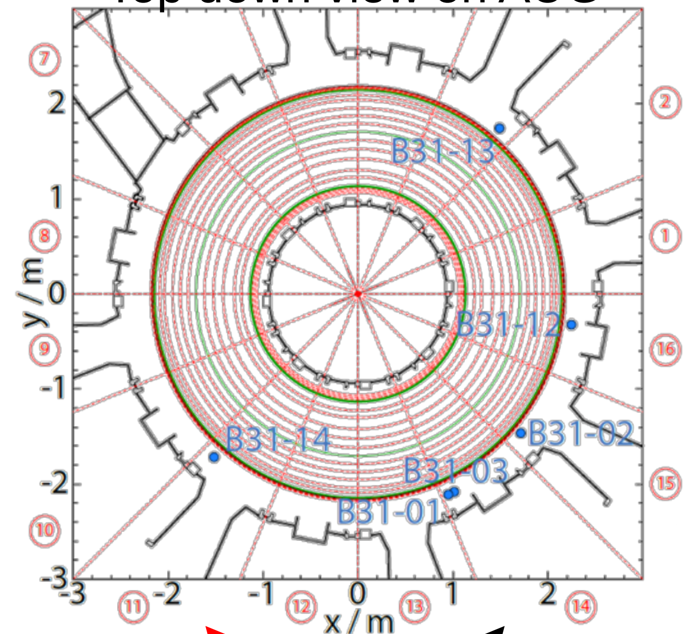

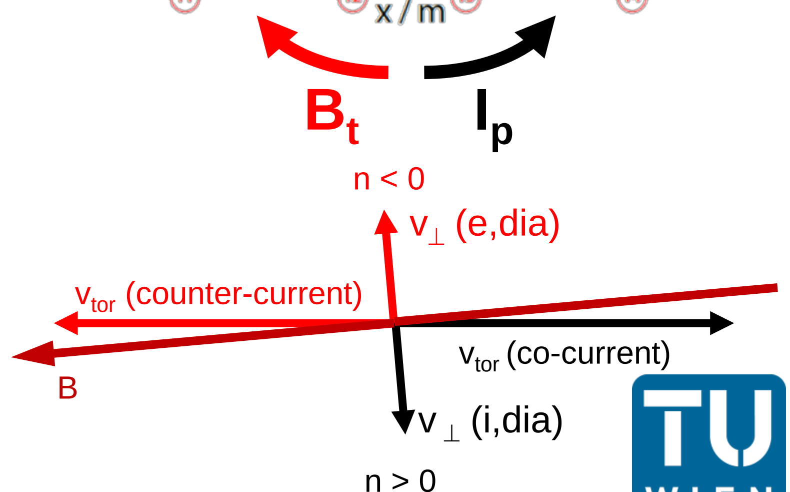

Mode number analysis

- Transfer functions of B_r coils are required

  [L. Horvath et al., PPCF 2015]

  - Especially for high toroidal mode numbers n and at high fluctuation frequencies

•Negative n:

- Counter-current propagation or propagation in electron diamagnetic direction

•Mode number fitted for every individual ELM cycle in time interval $\rightarrow$ fits superimposed $\rightarrow$ mode number histogram

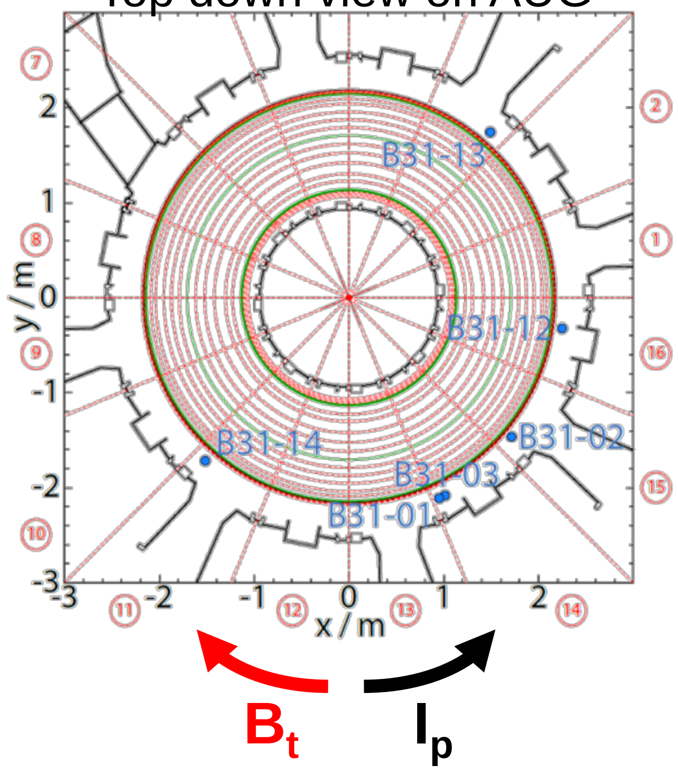

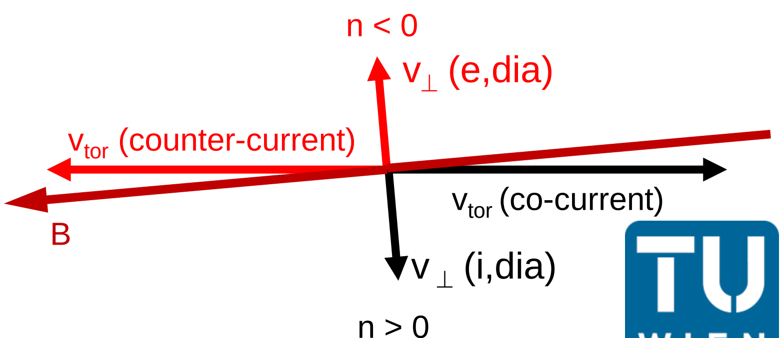

Similar n for both discharges

- In both cases n ~ -11 for the high frequency fluctuations
    - Similar mode structure
        - ➢ Different frequency due to different background $v_{E\times B}$

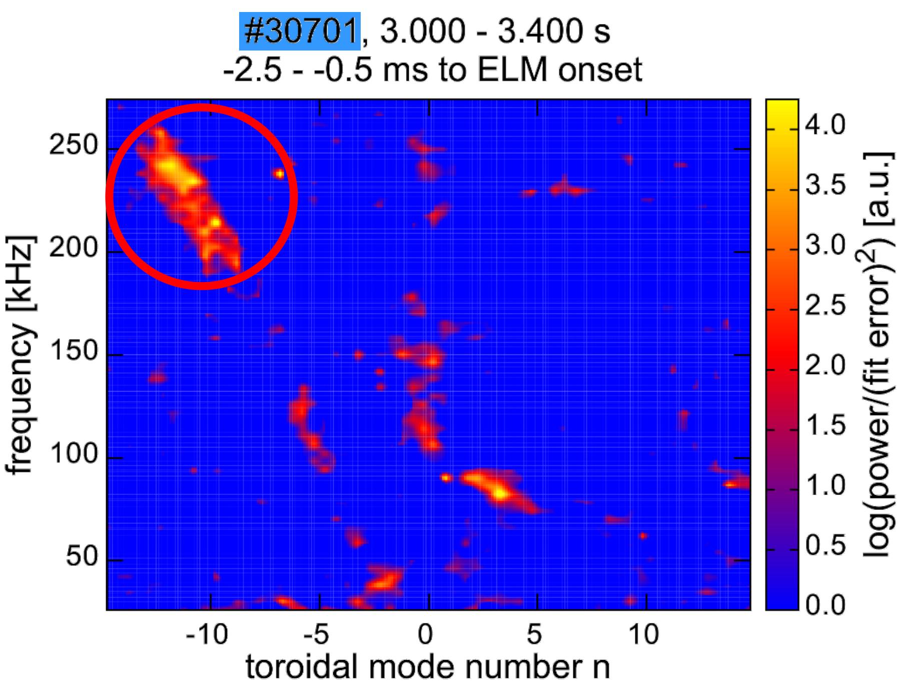

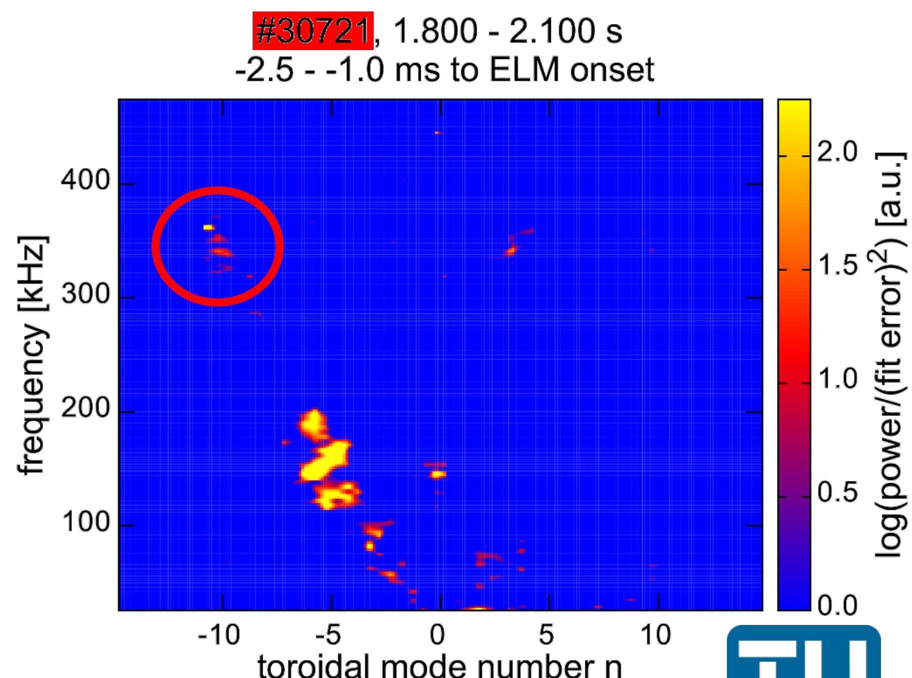

Similar n for both discharges

- In both cases n ~ -11 for the high frequency fluctuations
  - Similar mode structure
    - ➢ Different frequency due to different background $v_{E\times B}$
- Mode structure aligns with low frequency fluctuations < 200 kHz
  - Same propagation velocity → same location?

#30701, 3.000 - 3.400 s
-2.5 - -0.5 ms to ELM onset

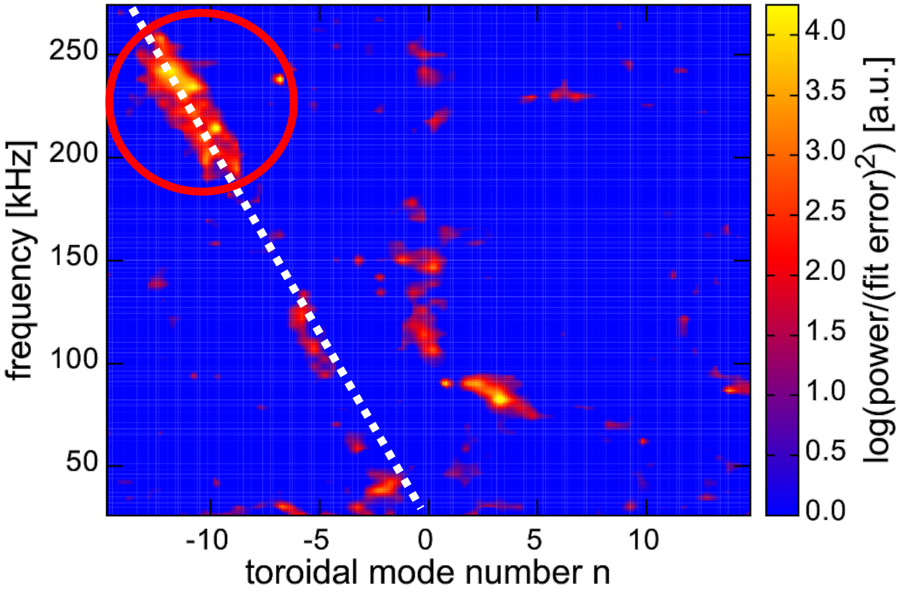

#30721, 1.800 - 2.100 s
-2.5 - -1.0 ms to ELM onset

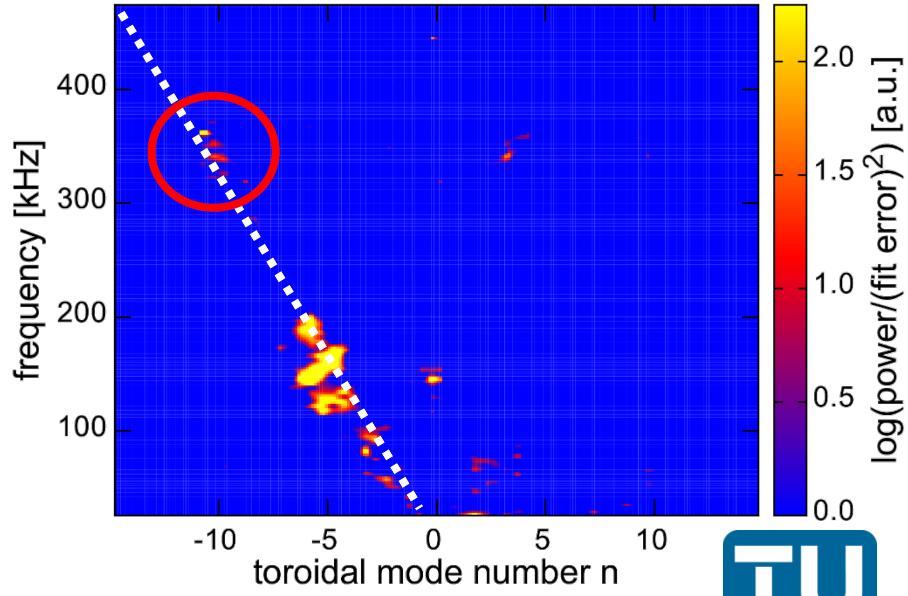

Fluctuations are seen on the HFS

- Fluctuation signature visible on the HFS
  - Similar onset as on the LFS
  - Same frequencies as on LFS

[F. M. Laggner et al., PPCF 2016]

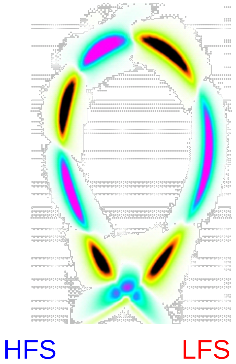

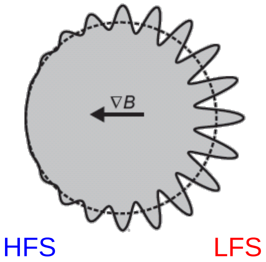

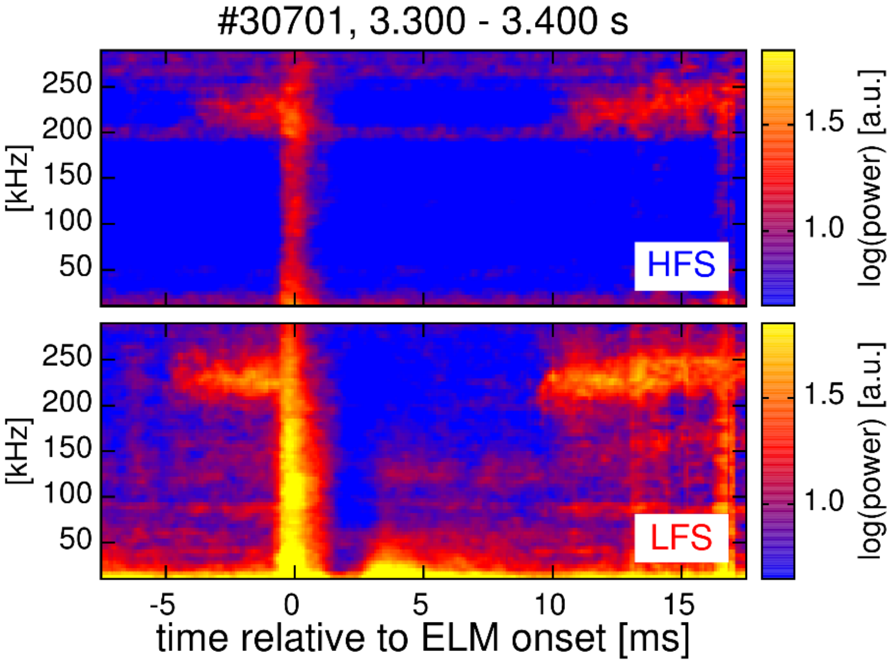

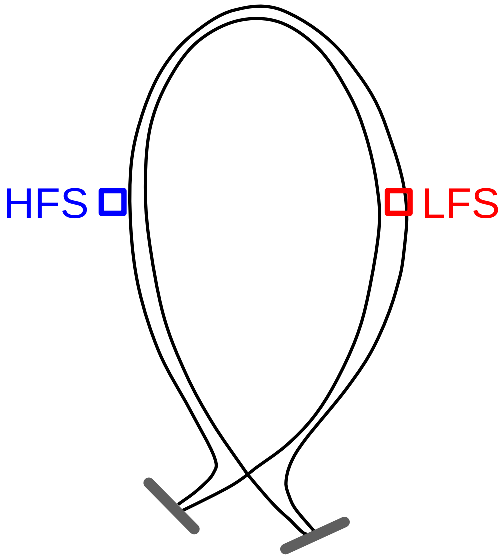

Fluctuations are seen on the HFS

- Fluctuation signature visible on the HFS
  - Similar onset as on the LFS
  - Same frequencies as on LFS

[F. M. Laggner et al., PPCF 2016]

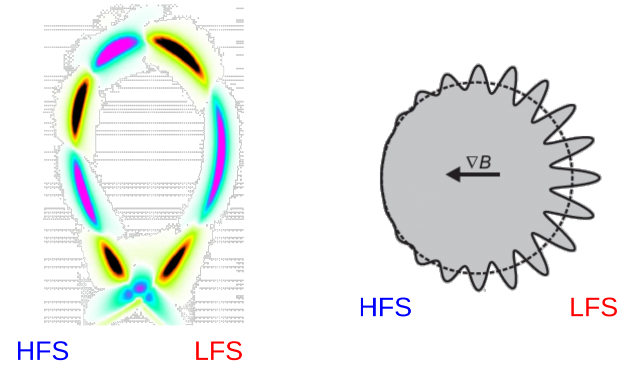

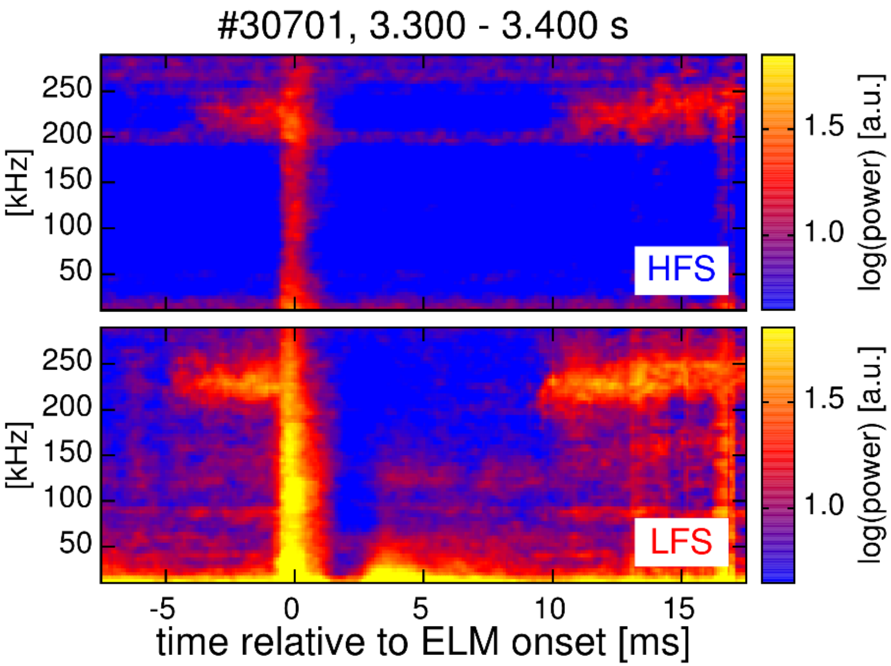

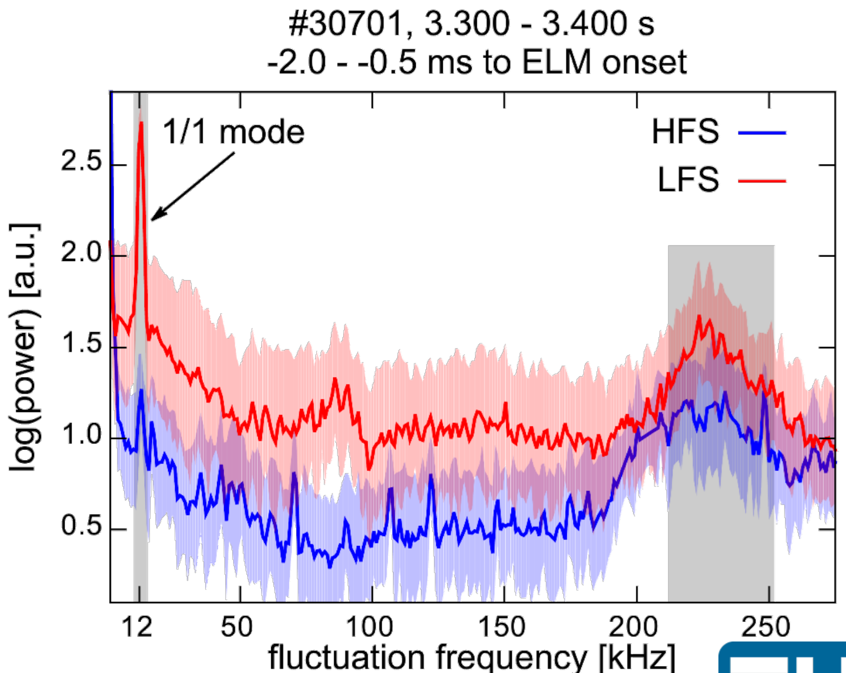

Fluctuations are seen on the HFS

- Fluctuation signature visible on the HFS
  - Similar onset as on the LFS
  - Same frequencies as on LFS

[F. M. Laggner et al., PPCF 2016]

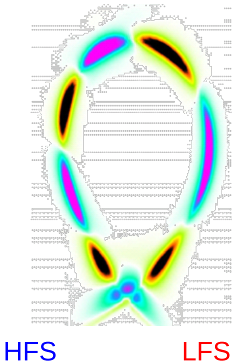

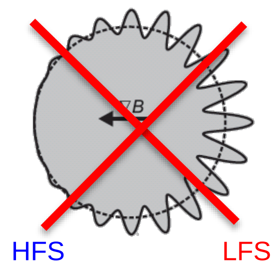

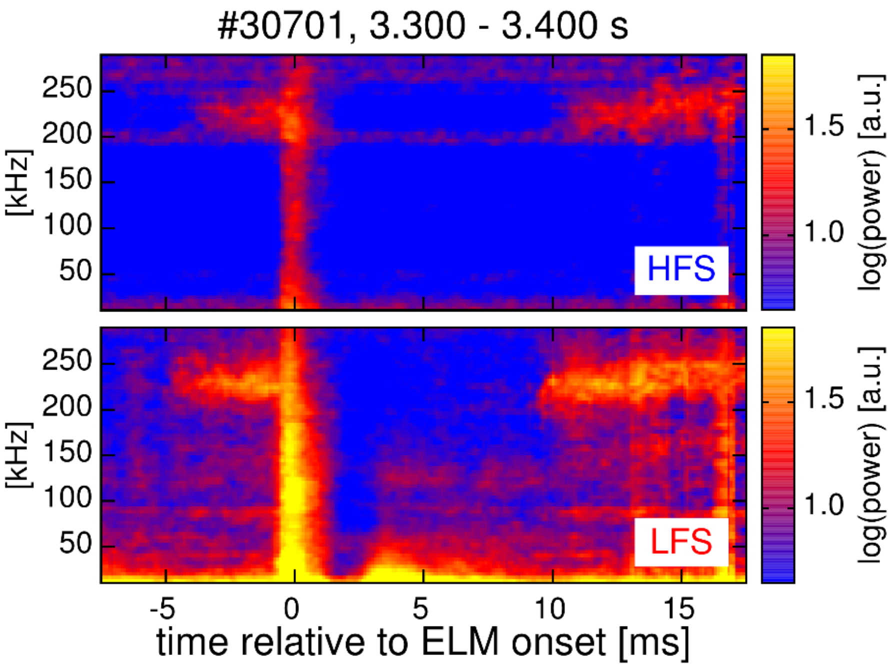

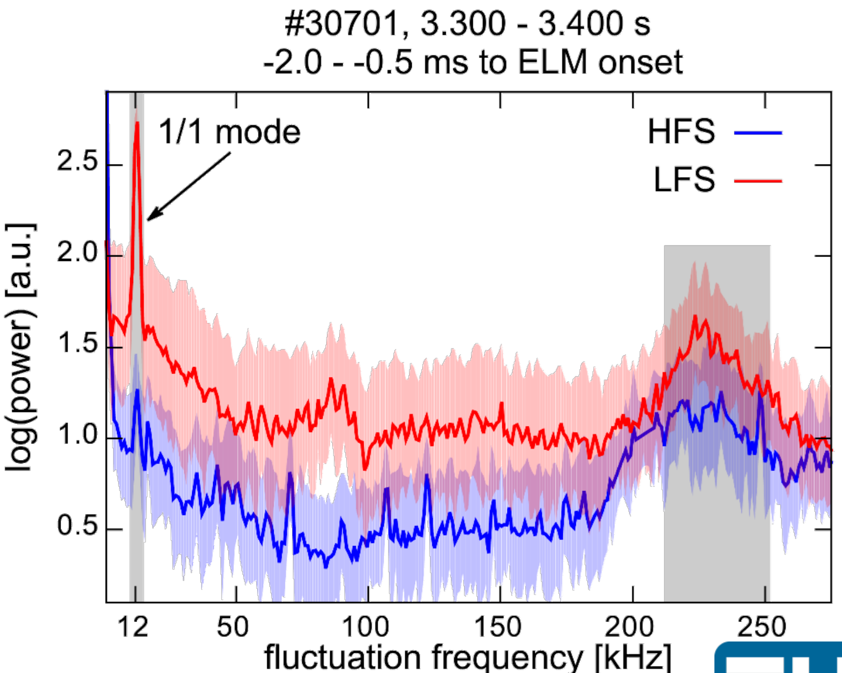

→ Supports large peeling component of mode structure

Linear ideal MHD stability analysis

- Investigate possible drives for instabilities (peeling vs. ballooning)
  - 3 phases with presence of high frequency fluctuations & clamped gradients

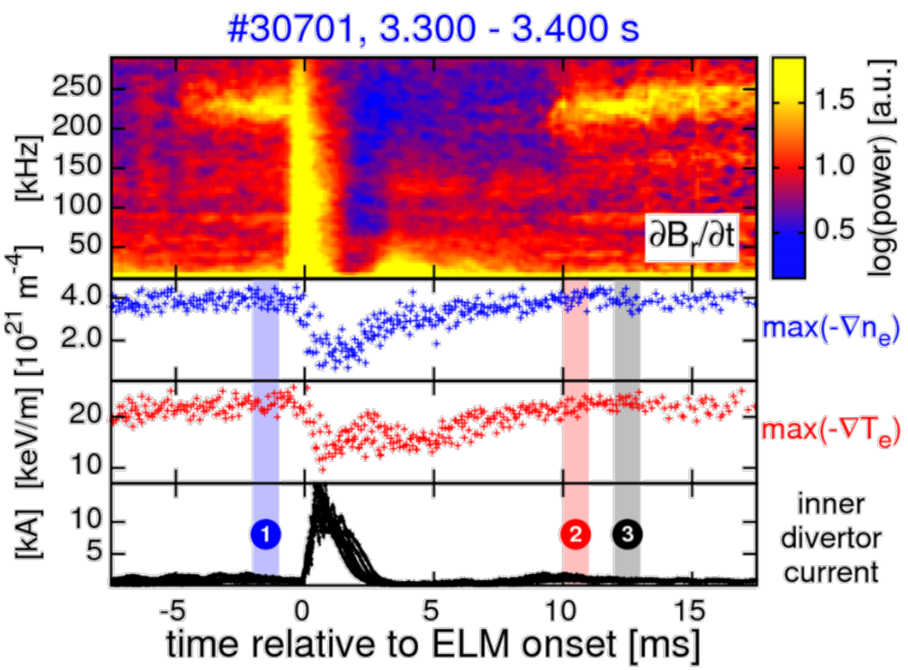

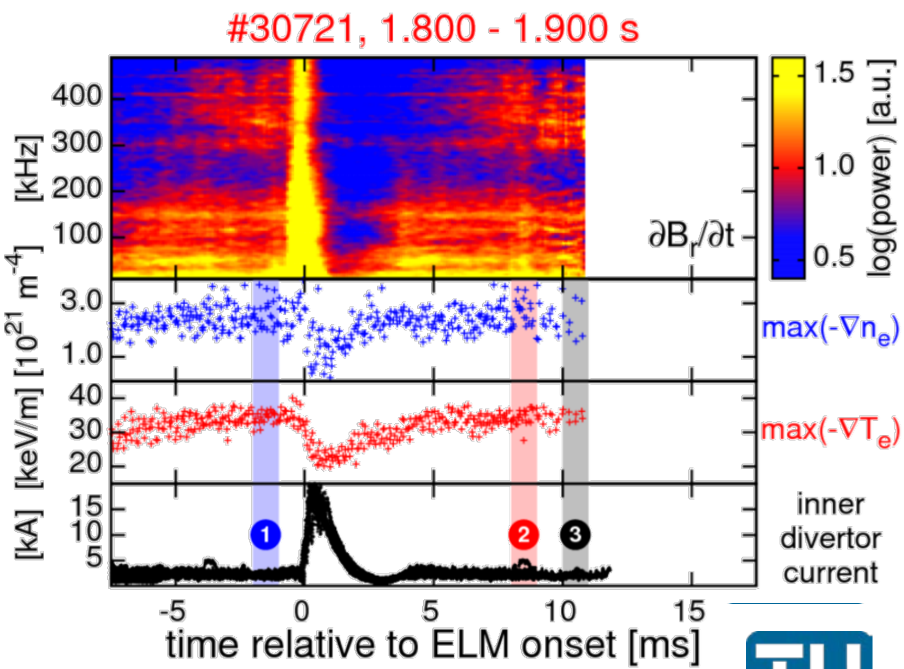

Linear ideal MHD stability analysis

- Investigate possible drives for instabilities (peeling vs. ballooning)
  - 3 phases with presence of high frequency fluctuations & clamped gradients
- No evolution of operational point
- No evolution of the stability boundary

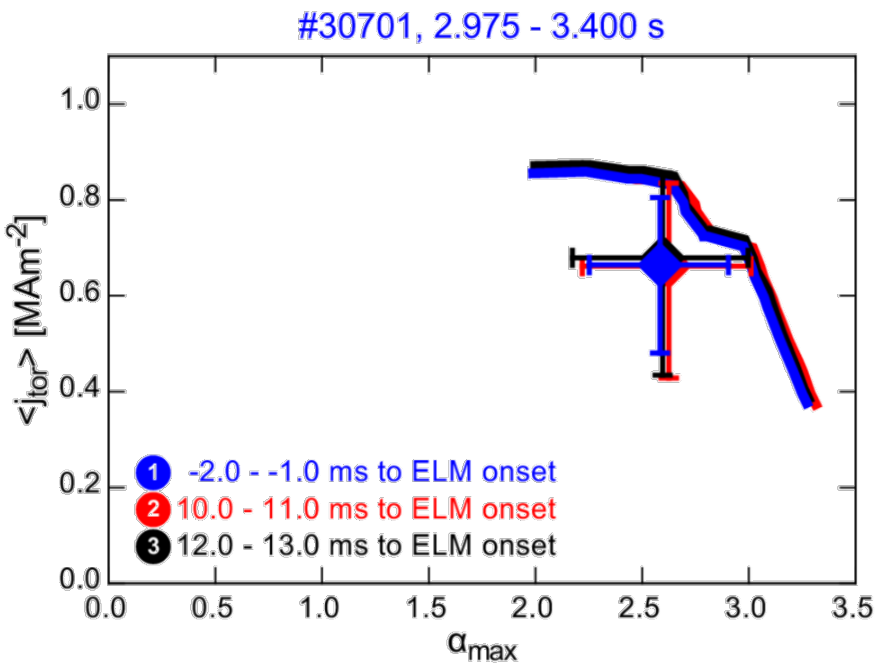

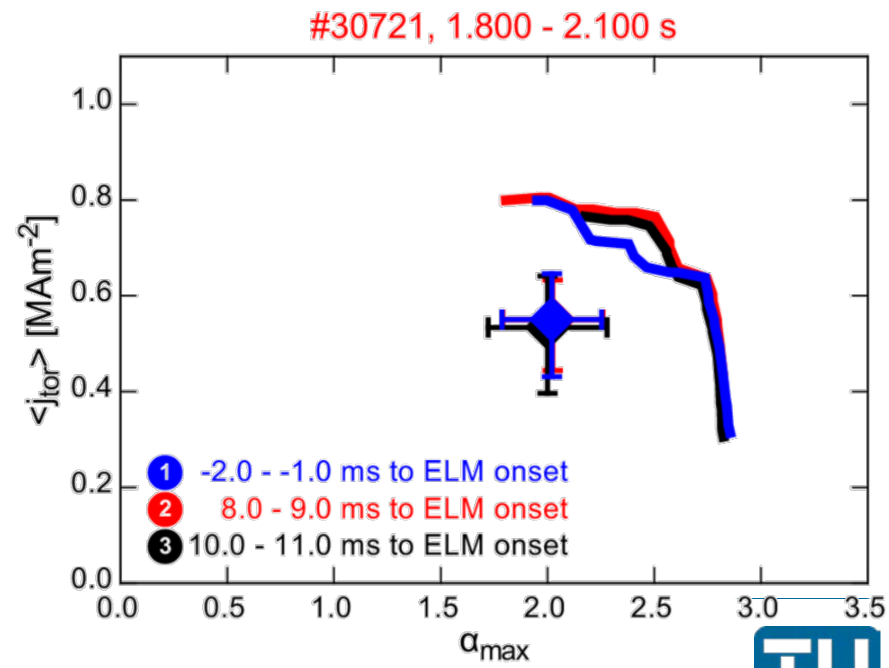

Linear ideal MHD stability analysis

- Investigate possible drives for instabilities (peeling vs. ballooning)
  - 3 phases with presence of high frequency fluctuations & clamped gradients
- No evolution of operational point
- No evolution of the stability boundary

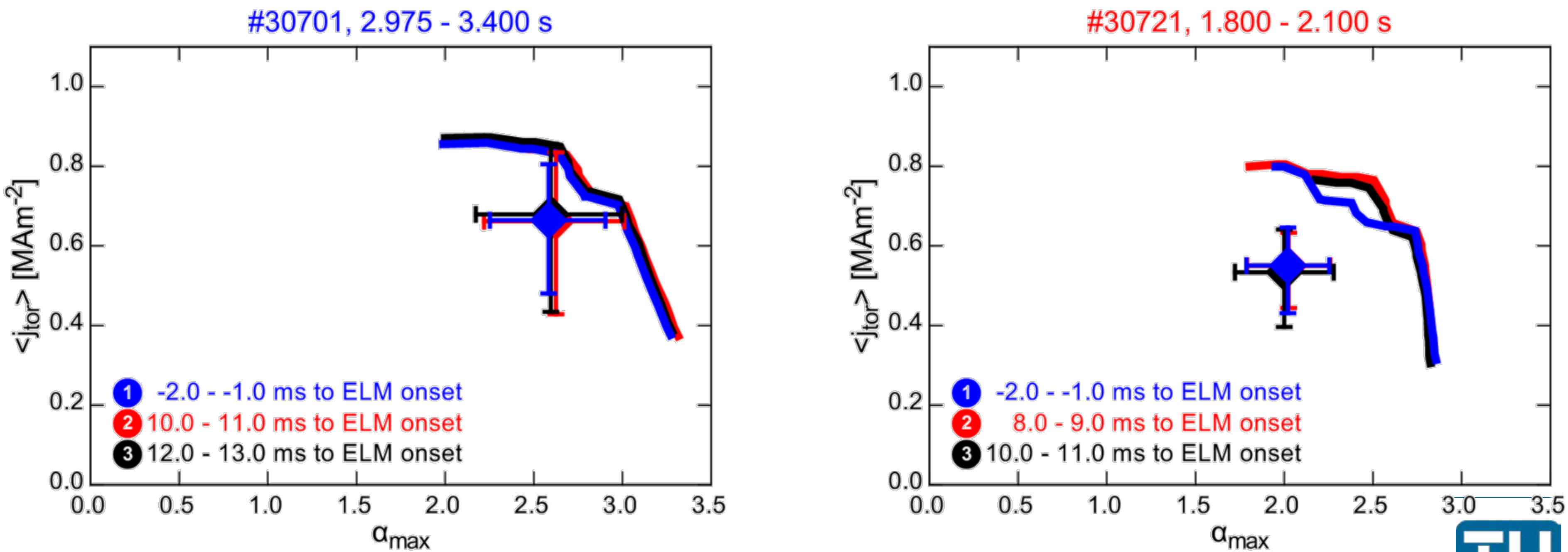

→ While high frequency fluctuations, pedestals consistent with P-B

Outline

- Introduction to pedestal stability
- Pedestal recovery and onset of magnetic fluctuations
  - Localization, poloidal and toroidal mode structure
- Comparison of the pedestal recovery for different main ion species
  - Similar sequence of recovery phases in different species
- Connecting the evolution of the outer divertor to the pedestal recovery
  - High recycling regime connected to density evolution
- Summary & conclusions

Pedestal top match in D and H

- Match of the edge profiles
  - $I_p \sim 1.0$ MA, $B_t \sim -2.5$ T, $q_{95} \sim 3.8$

➢ factor of ~2 higher heating power in H

➢ factor of ~10 higher gas fueling rates in H required

➢ Steeper pedestal ne profile in D

D

gas puff
$1.5 \cdot 10^{21}$ s^{-1}

P_{heat}
~3.9 MW

H

gas puff
$12 \cdot 10^{21}$ s^{-1}

P_{heat}
~7.5 MW

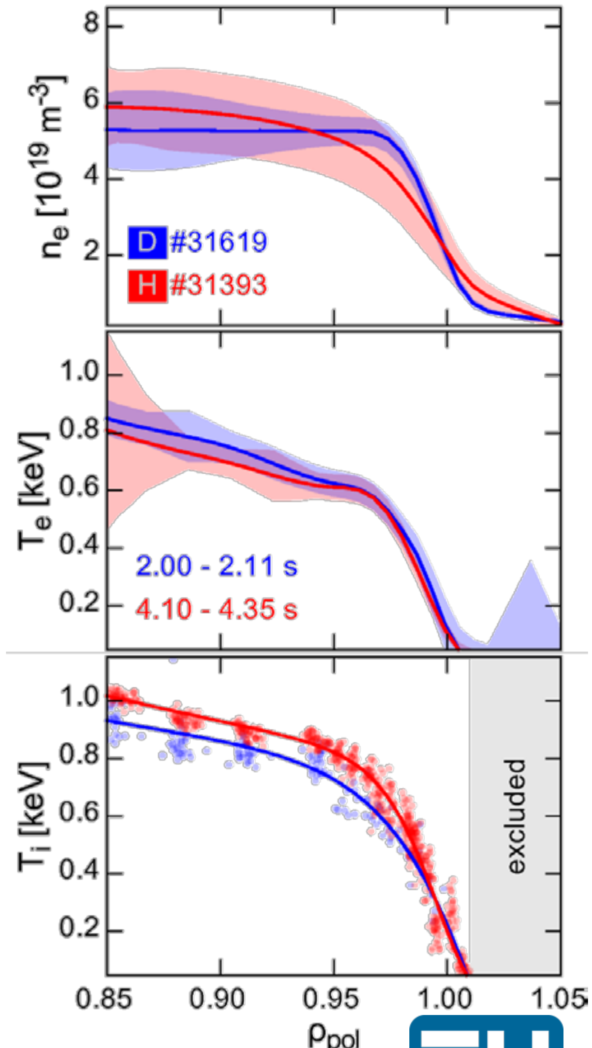

He discharges

- Main ion density (n_i) ~ 0.5 n_e

- When comparable n_e to D and H
  - ELM free
    - ➢ Edge pressure gradient not critical

- Higher pedestal top n_e required to get ELMs

He

gas puff
$0.1 \cdot 10^{21}$ s^{-1}

P_{heat}
~8.5 MW

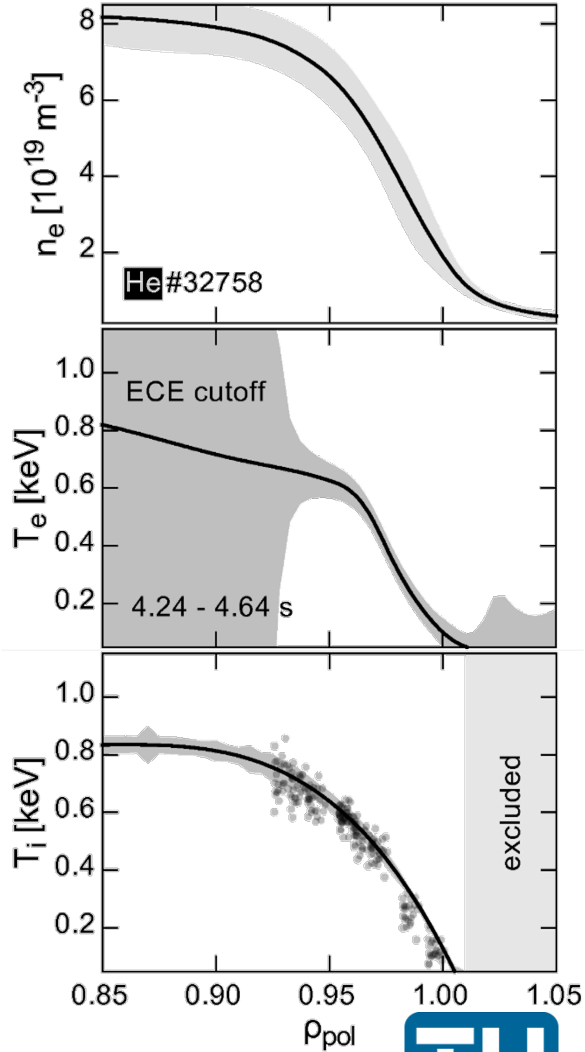

Inter-ELM pedestal evolution similar

- Pedestal recovery phases
  1) n_e pedestal (Δt_{ne})
  2) T_e pedestal (Δt_{Te})

- Different timescales
  - attributed to changes in P_{heat}, gas puff and neutral velocity

- T_i evolves on timescale of n_e

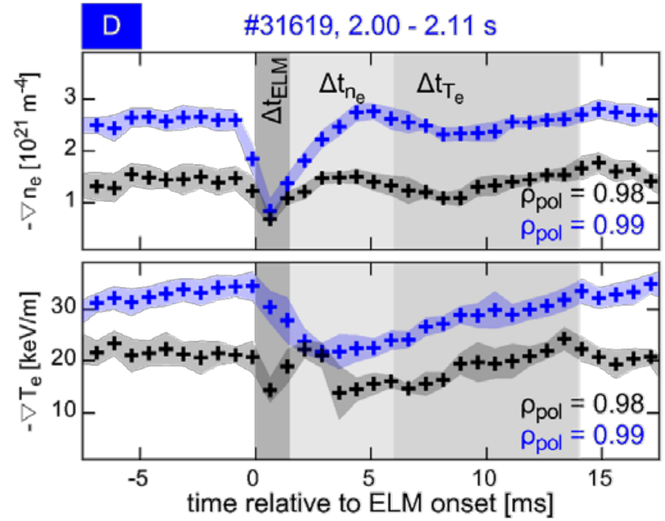

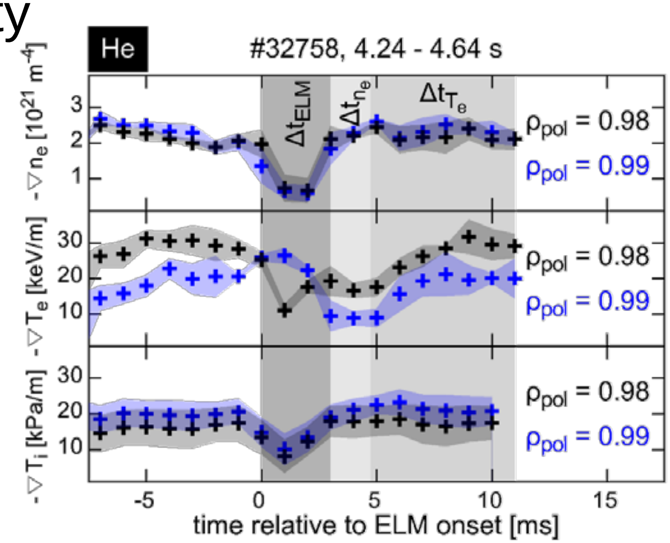

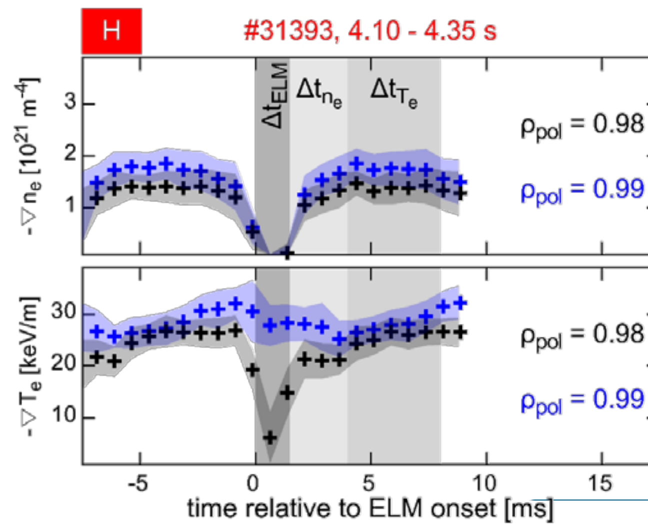

Inter-ELM pedestal evolution similar

- Pedestal recovery phases
  1) n_e pedestal (Δt_{ne})
  2) T_e pedestal (Δt_{Te})

- Different timescales
  - attributed to changes in P_{heat}, gas puff and neutral velocity

- T_i evolves on timescale of n_e

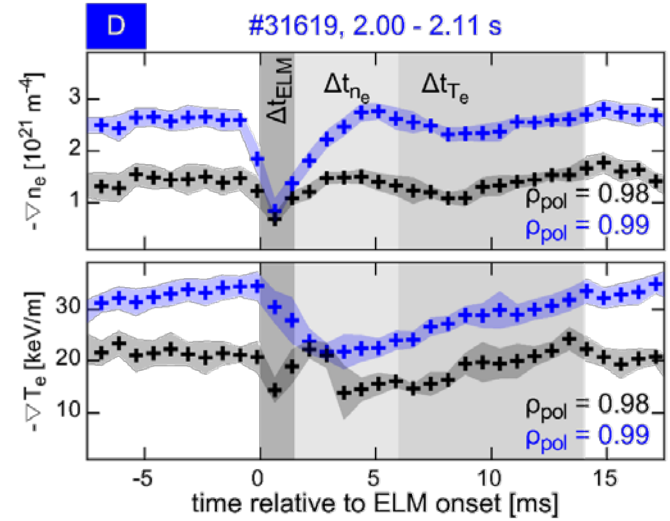

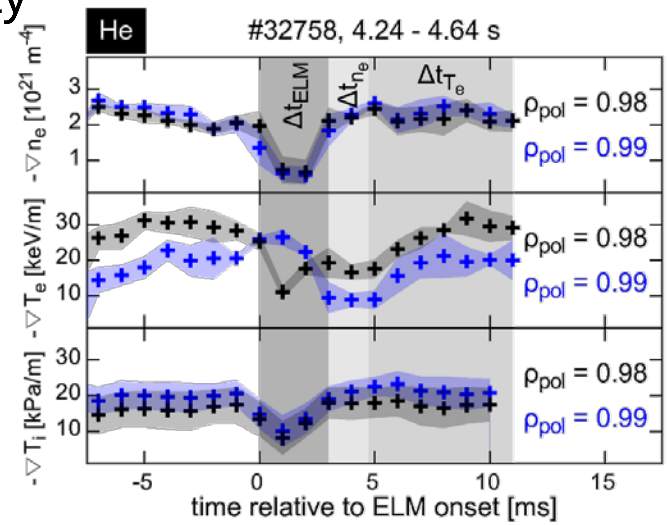

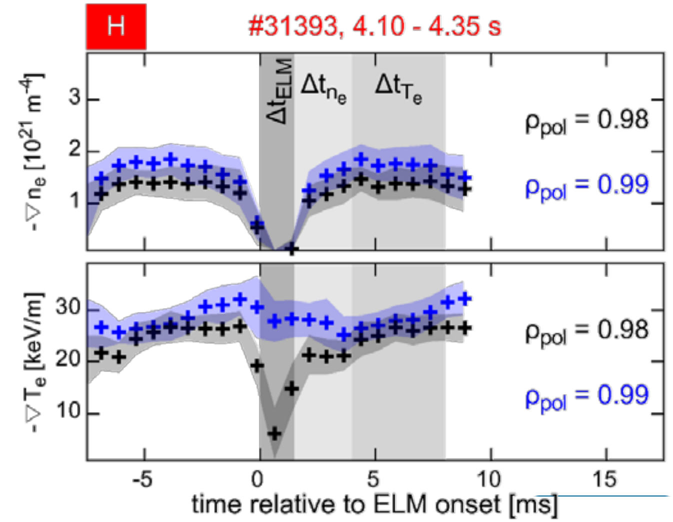

→ Indication for similar mechanisms acting in the pedestal recovery

Pre-ELM toroidal mode structures

- Negative n:
  - Similar to the one observed in the $\nu^*_{e,ped}$ variation
- Two mode number branches with similar n
  [F. Mink et al., accepted in PPCF]
- Slope represents different rotation velocity relative to the lab frame

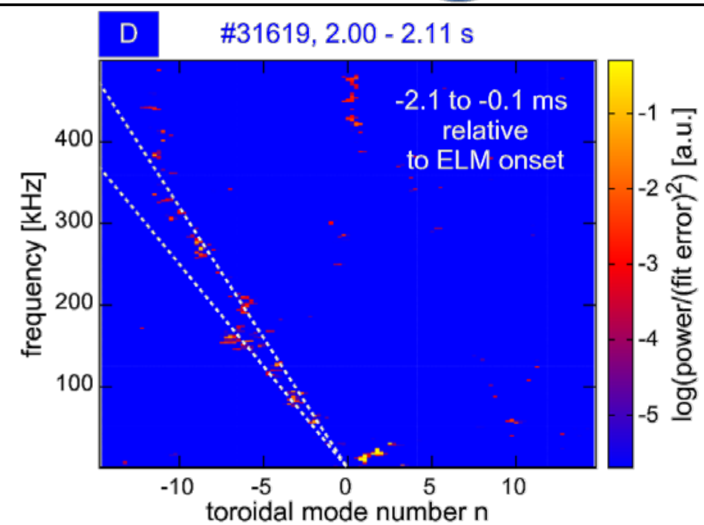

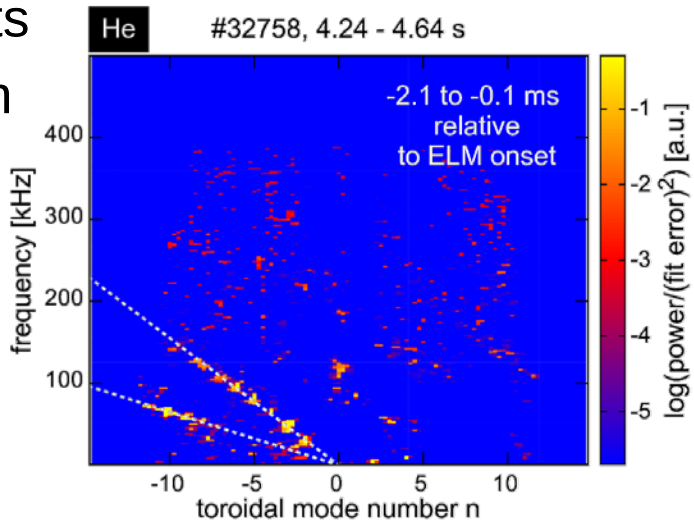

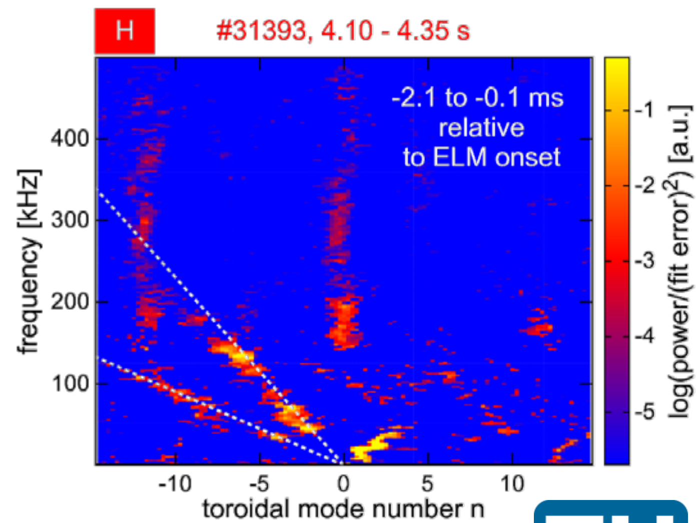

Pre-ELM toroidal mode structures

- Negative n:
  - Similar to the one observed in the $\nu^*_{e,ped}$ variation
- Two mode number branches with similar n
  [F. Mink et al., accepted in PPCF]
- Slope represents different rotation velocity relative to the lab frame

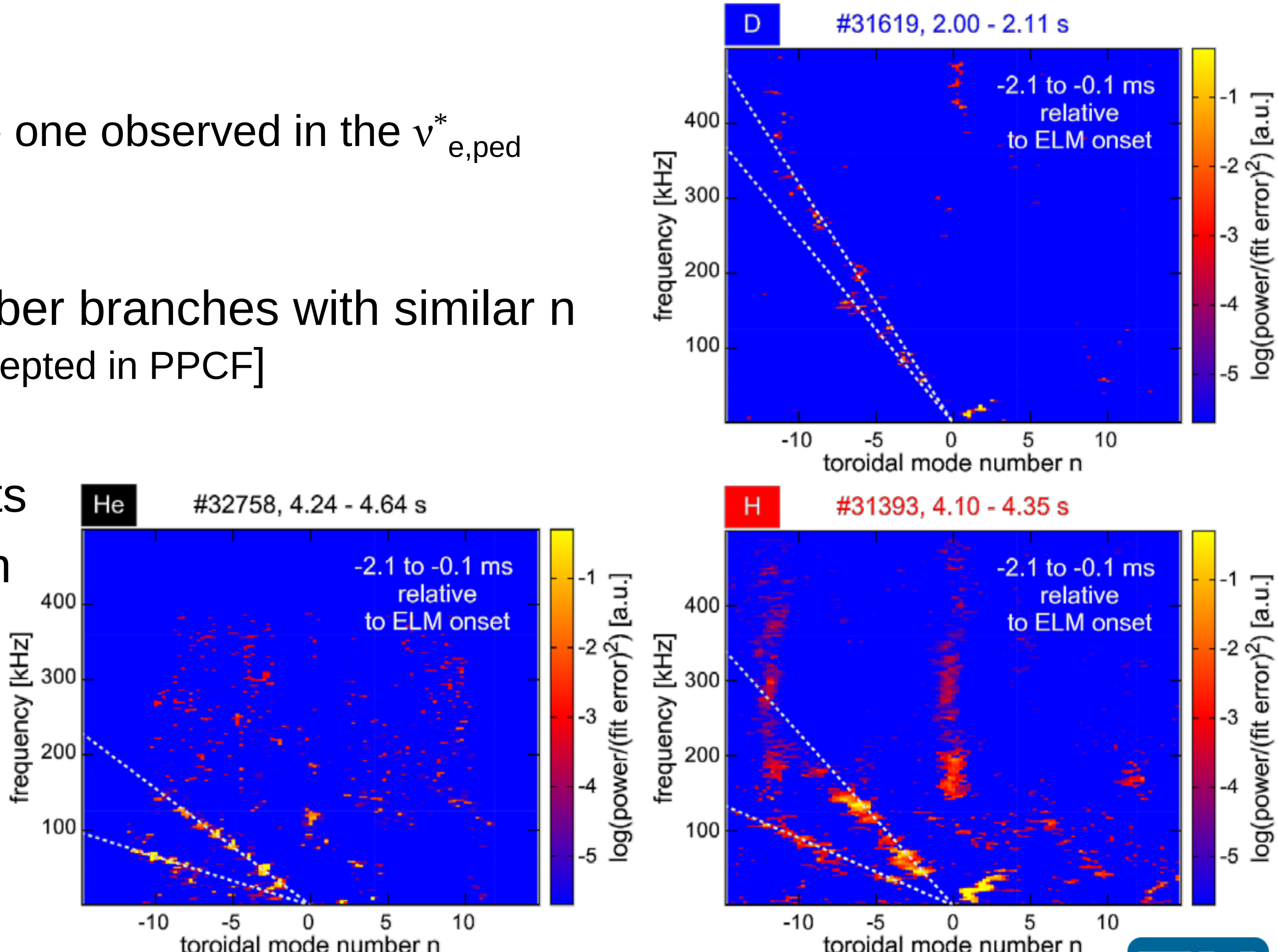

→ E×B velocity affected by changes in ∇n_e

Frequencies consistent with E×B

- Data from pedestal parameter variation
    - Selected to span wide range of $\nabla p_e/en_e$
- Transformed into E×B velocity

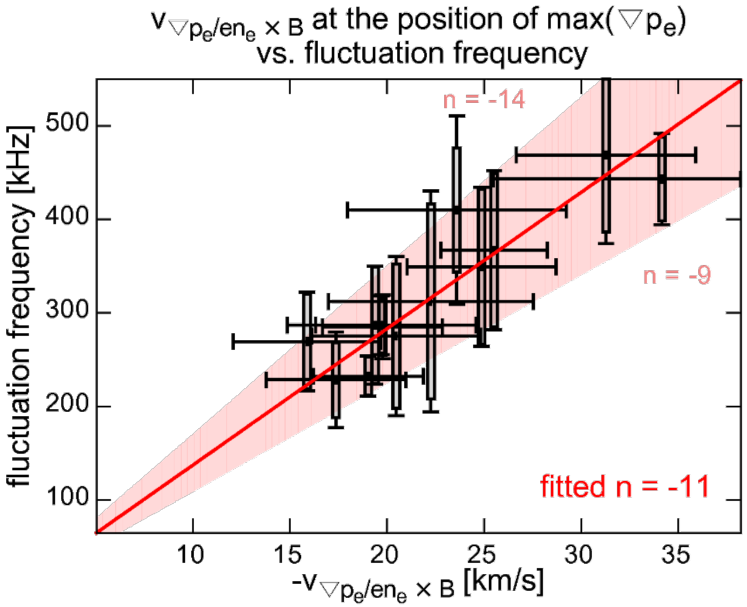

[F. M. Laggner et al., PPCF 2016]

Frequencies consistent with E×B

- Data from pedestal parameter variation
  - Selected to span wide range of $\nabla p_e/en_e$
- Transformed into E×B velocity

→ D,H and He plasmas have different rotation, therefore detected frequency is different

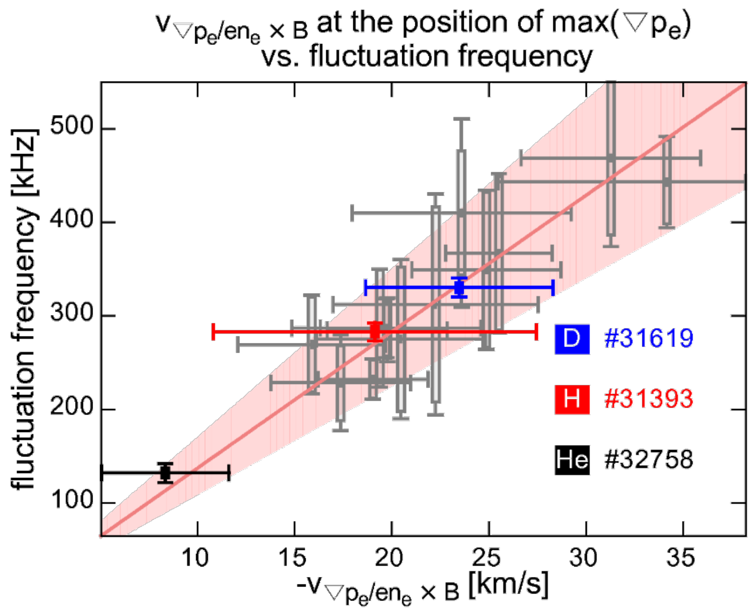

Outline

- Introduction to pedestal stability

- Pedestal recovery and onset of magnetic fluctuations
  - Localization, poloidal and toroidal mode structure

- Comparison of the pedestal recovery for different main ion species
  - Similar sequence of recovery phases in different species

- Connecting the evolution of the outer divertor to the pedestal recovery
  - High recycling regime connected to density evolution

- Summary & conclusions

Change of the divertor conditions

- Outer divertor in high recycling regime after the ELM crash
- Occurrence depends on the gas puff

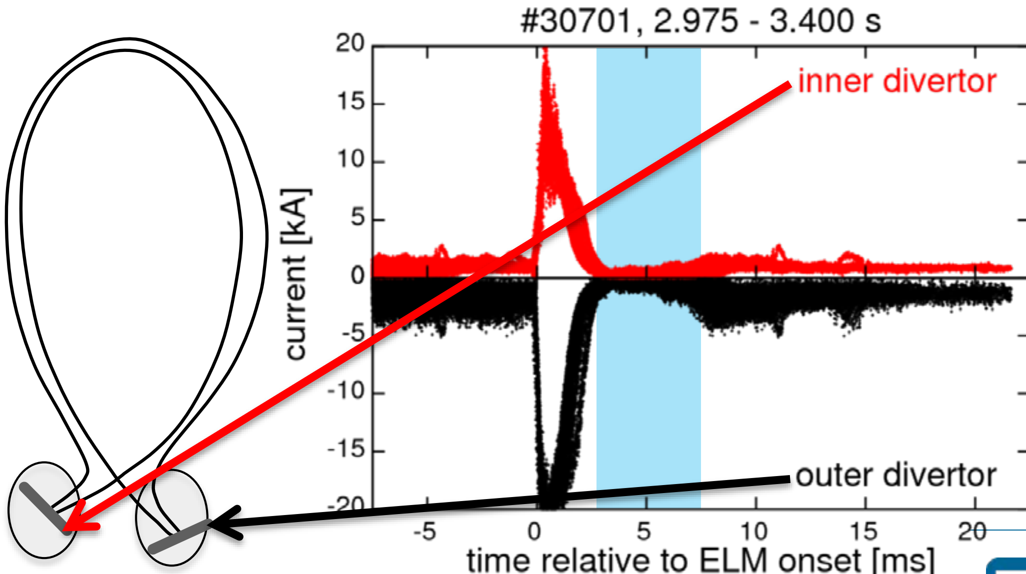

Change of the divertor conditions

- Outer divertor in high recycling regime after the ELM crash
  [M. Wischmeier et al., JNM 2007]
- Occurrence depends on the gas puff

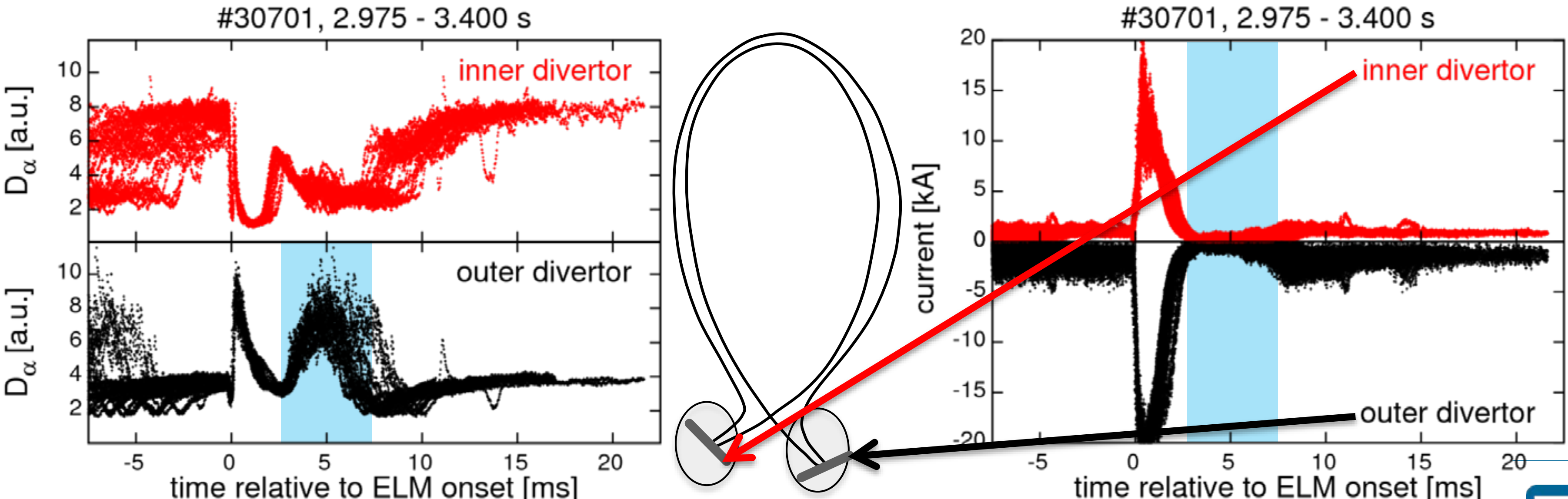

Change of the divertor conditions

- Outer divertor in high recycling regime after the ELM crash
  [M. Wischmeier et al., JNM 2007] [S. Brezinsek et al., Phys. Scr. 2016]
- Occurrence depends on the gas puff
- Post-ELM n_e increase at the outer target

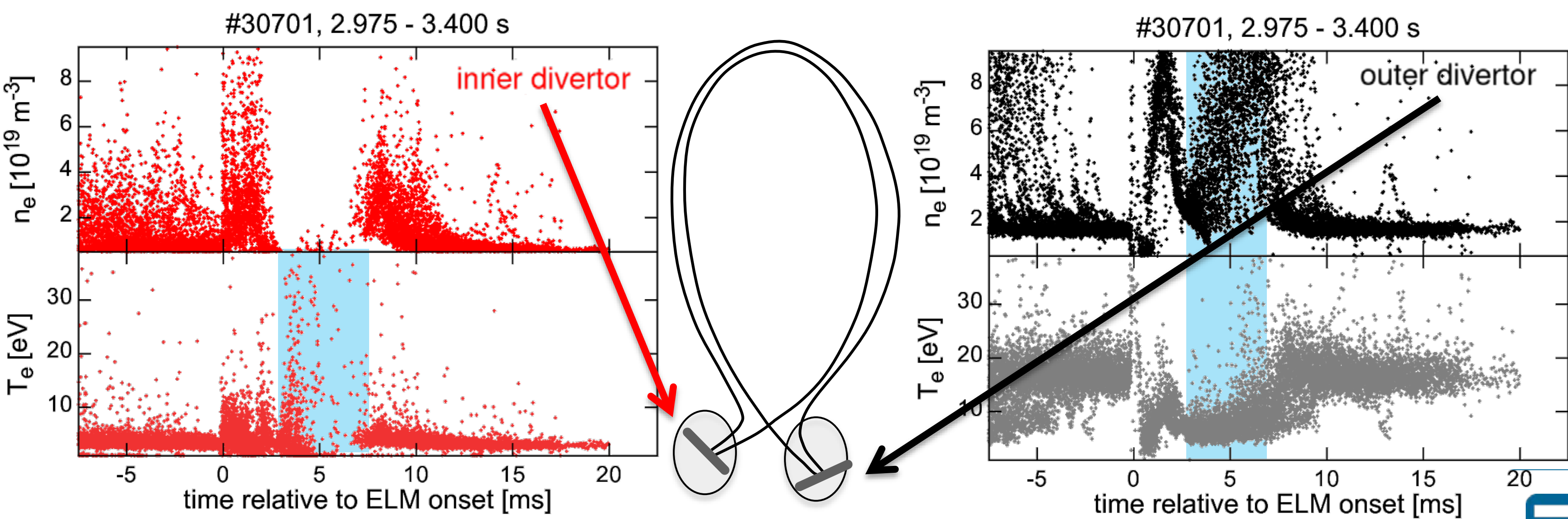

Connecting divertor to pedestal

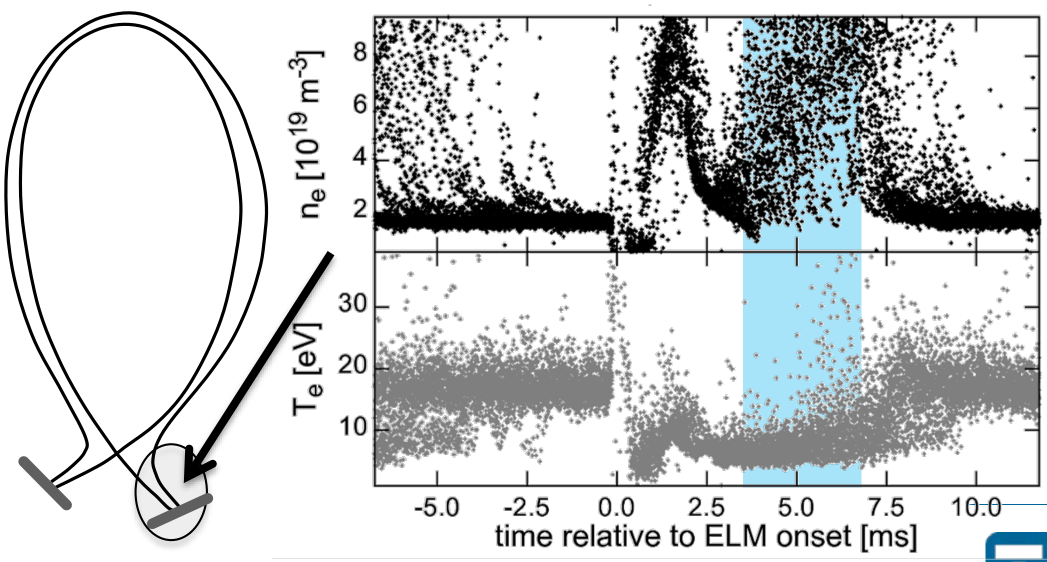

Connecting divertor to pedestal

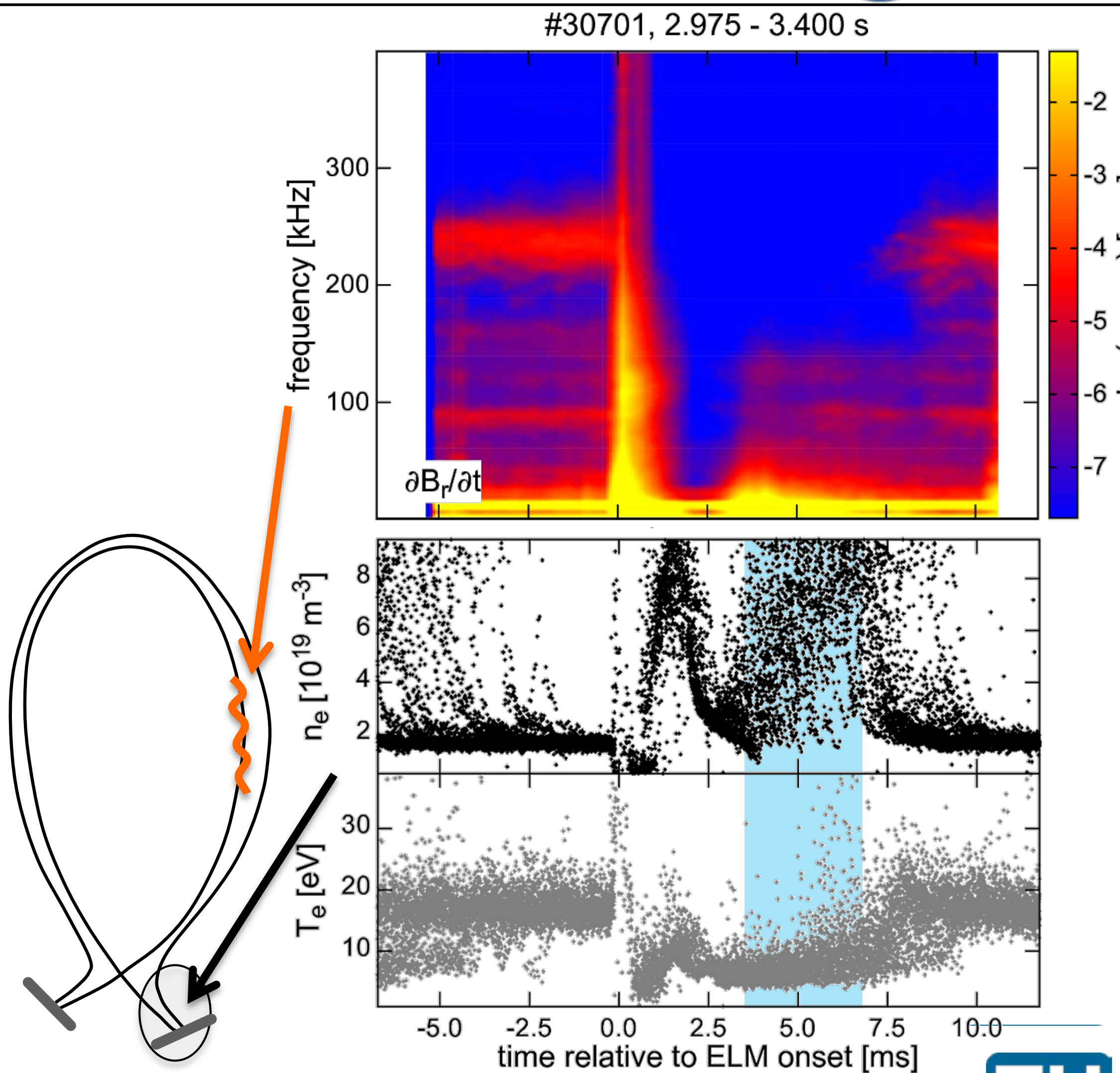

Connecting divertor to pedestal

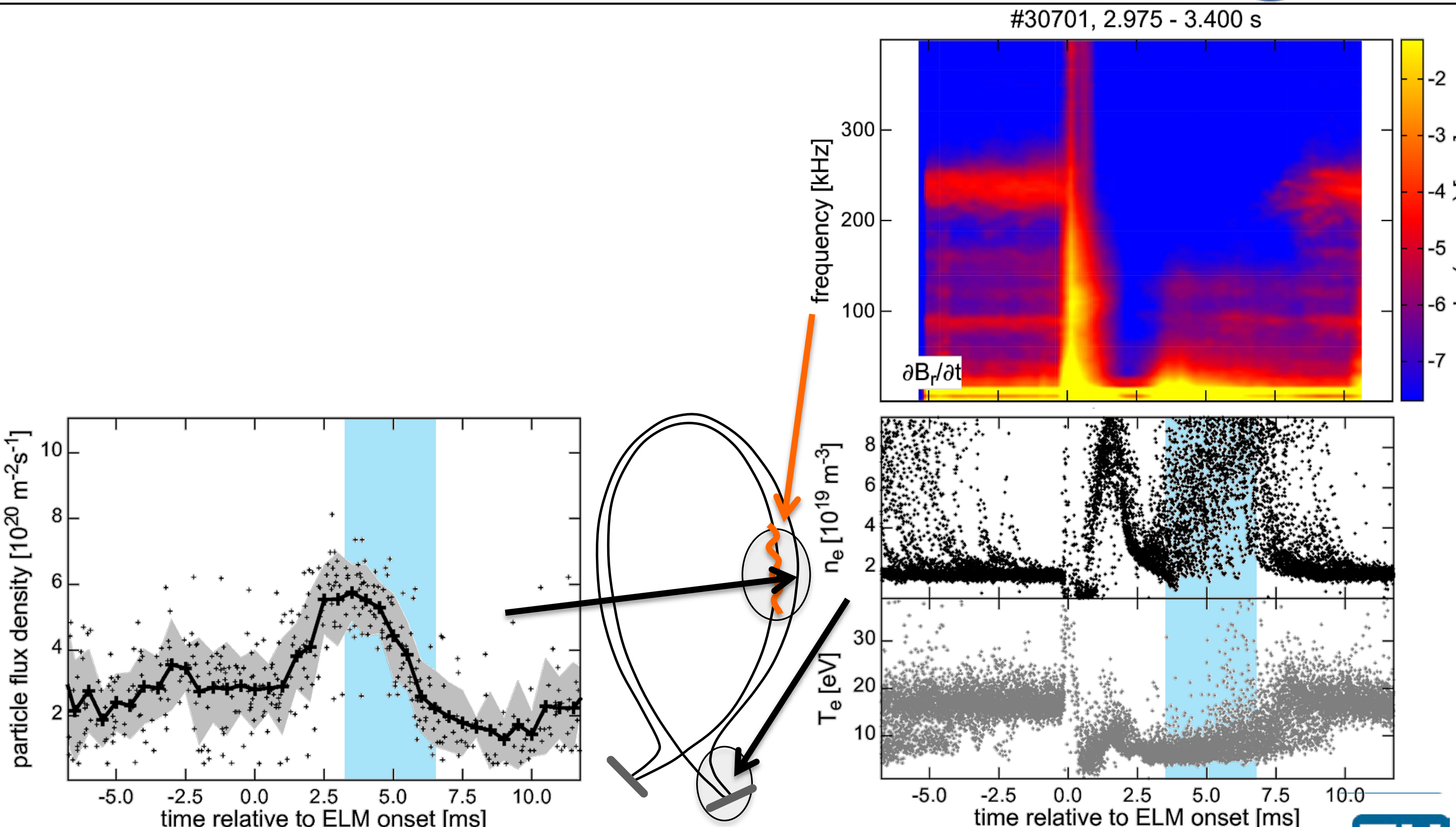

Connecting divertor to pedestal

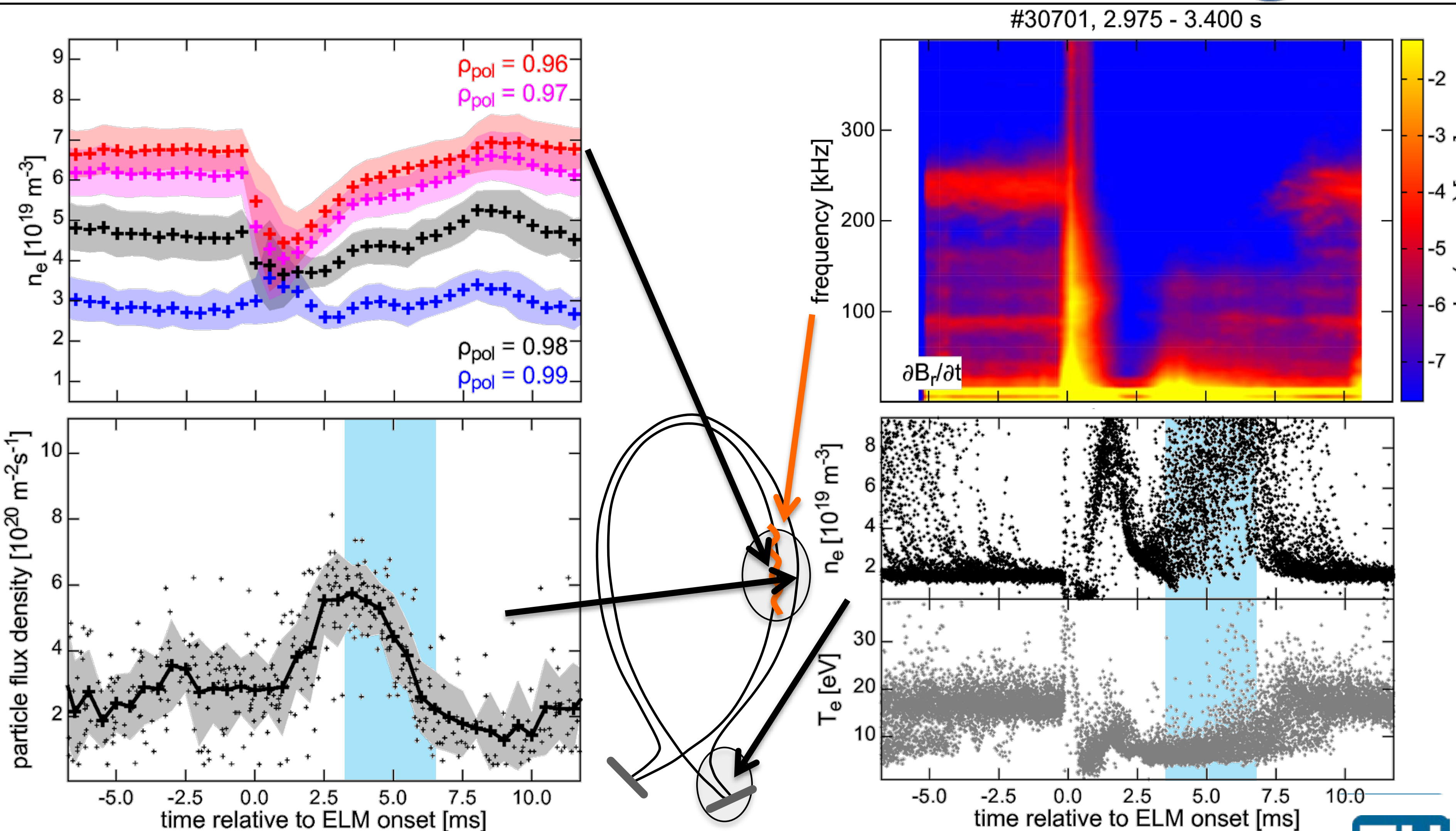

Simple 1D-estimation of transport

- Continuity equation:

$$\frac{\partial n}{\partial t} = -\frac{\partial \Gamma}{\partial x} + \alpha S_i$$

- Estimation of the source (S_i) by 1D neutral transport code KN1D

  [B. LaBombard, PSFC report 2000]

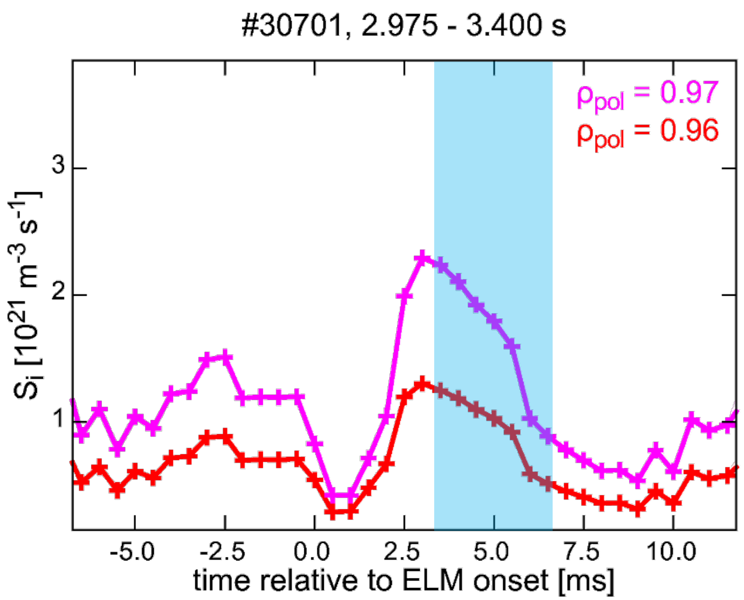

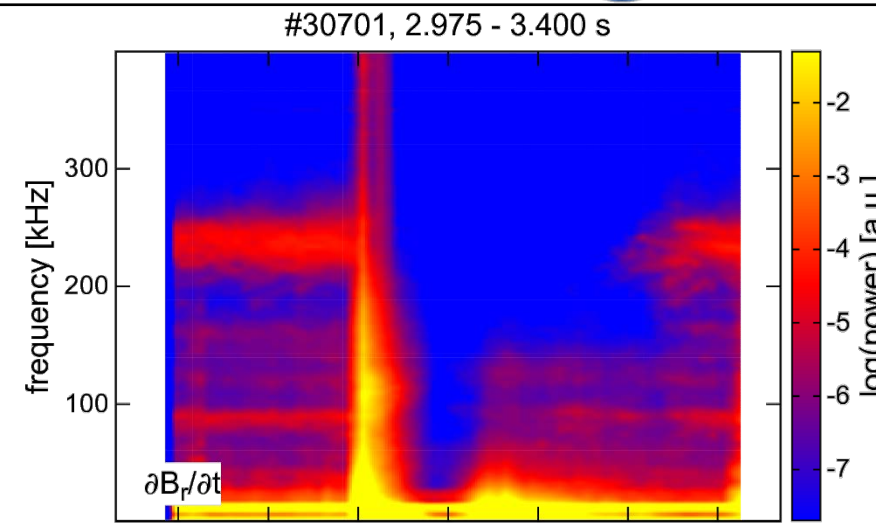

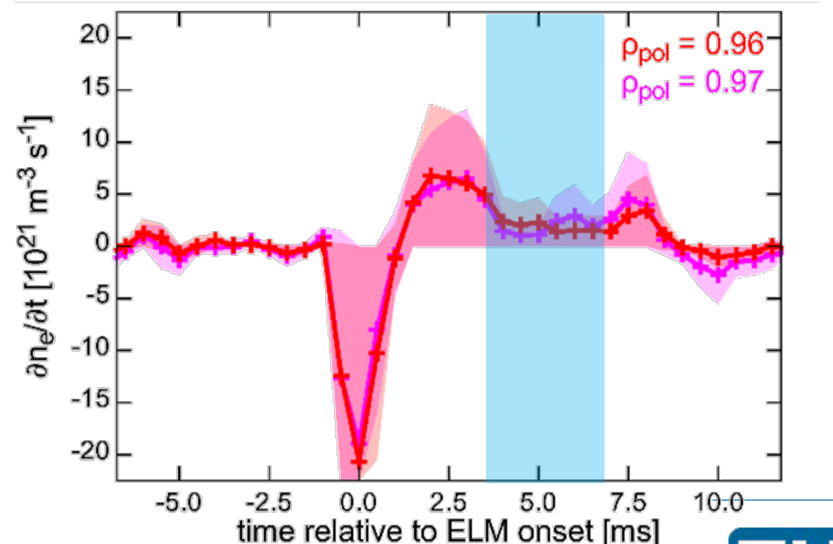

Particle transport dynamic after ELM

- Continuity equation:

$$\frac{\partial n}{\partial t} = -\frac{\partial \Gamma}{\partial x} + \alpha S_i$$

- Diffusive particle flux assumed

$$\Gamma = -D\frac{\partial n}{\partial x}$$

- Prior ELM
  - reference scale for S_i
    - D assumed 0.25 m^2/s (ρ_{pol} 0.96)
    - Determination of α
- Post ELM
  - D significantly decreases when magnetic activity is low
  - D increase when fluctuations set in

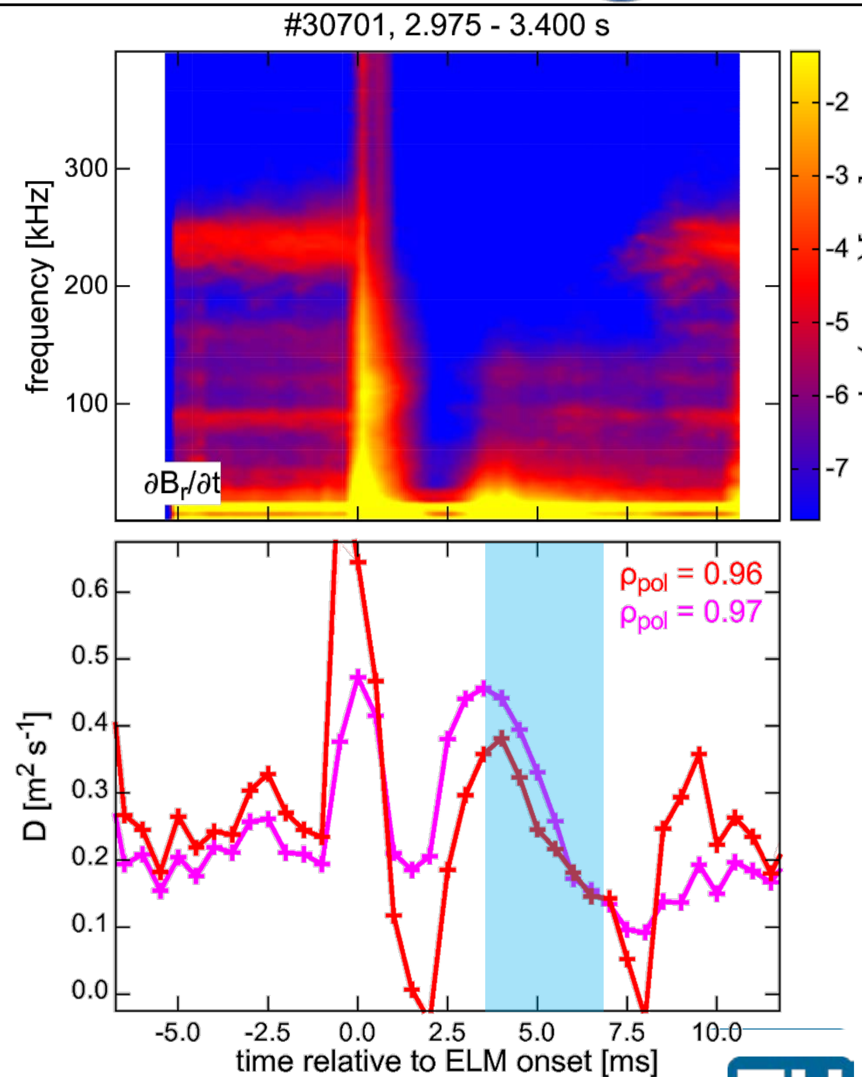

Particle transport dynamic after ELM

- Continuity equation:

$$\frac{\partial n}{\partial t} = -\frac{\partial \Gamma}{\partial x} + \alpha S_i$$

- Diffusive particle flux assumed

$$\Gamma = -D\frac{\partial n}{\partial x}$$

- Prior ELM
  - reference scale for S_i
    - ➢ D assumed 0.25 m^2/s (ρ_{pol} 0.96)
    - ➢ Determination of α
- Post ELM
  - D significantly decreases when magnetic activity is low
  - D increase when fluctuations set in

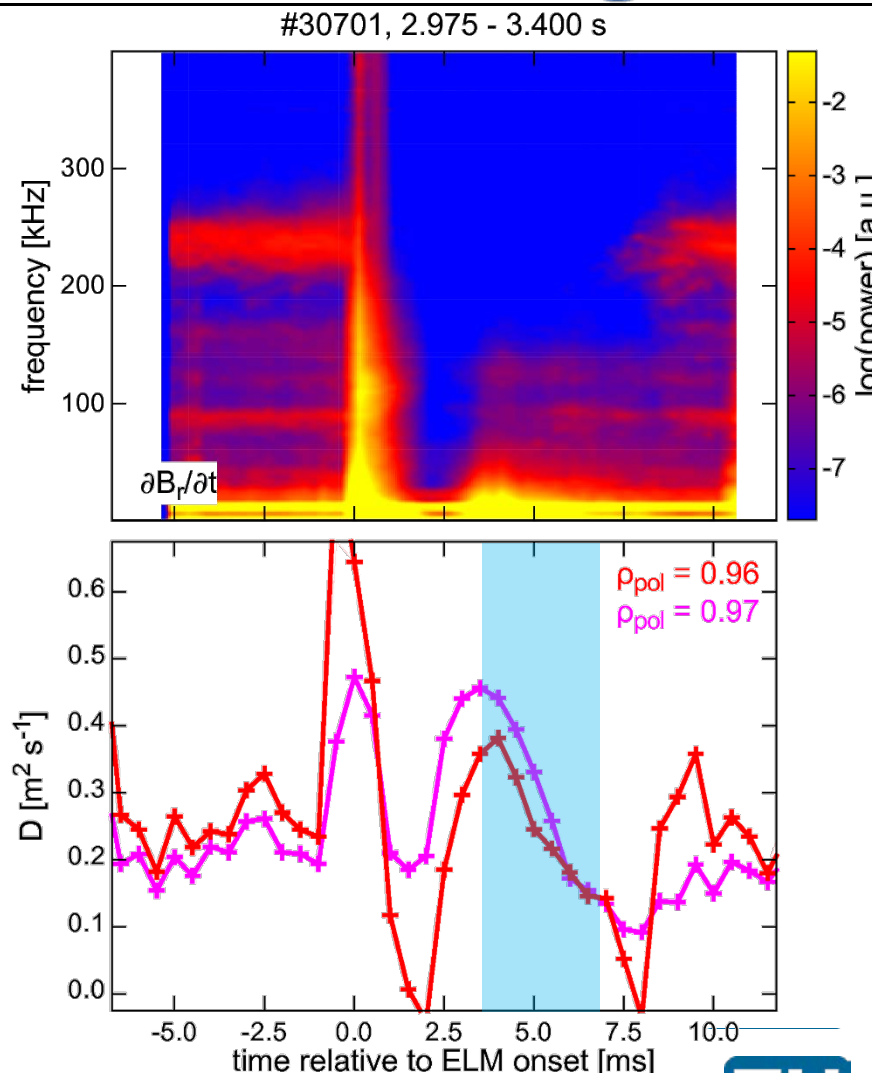

→ Indication for change of particle transport

Summary & conclusions

- Magnetic fluctuations correlated with pedestal evolution
  - Onset correlated to the recovery of $T_{e,ped}$ (clamping of ∇n_e and ∇T_e)
  - Detected frequency scales with background velocity
  - Toroidal mode structure with n ~ -11 in all investigated cases
  - Fluctuations are detectable on the HFS
    - ➢ Instability located in the steep gradient region, large scale toroidal structure with significant peeling component

Summary & conclusions

- Magnetic fluctuations correlated with pedestal evolution
  - Onset correlated to the recovery of $T_{e,ped}$ (clamping of ∇n_e and ∇T_e)
  - Detected frequency scales with background velocity
  - Toroidal mode structure with n ~ -11 in all investigated cases
  - Fluctuations are detectable on the HFS
    - ➢ Instability located in the steep gradient region, large scale toroidal structure with significant peeling component

- Identified in D, H and He plasmas
  - Similar sequence pedestal recovery phases
  - Pre-ELM toroidal mode structure comparable
    - ➢ Mechanisms in pedestal recovery independent of main ion species

Summary & conclusions

- Magnetic fluctuations correlated with pedestal evolution
  - Onset correlated to the recovery of $T_{e,ped}$ (clamping of ∇n_e and ∇T_e)
  - Detected frequency scales with background velocity
  - Toroidal mode structure with n ~ -11 in all investigated cases
  - Fluctuations are detectable on the HFS
    - ➢ Instability located in the steep gradient region, large scale toroidal structure with significant peeling component

- Identified in D, H and He plasmas
  - Similar sequence pedestal recovery phases
  - Pre-ELM toroidal mode structure comparable
    - ➢ Mechanisms in pedestal recovery independent of main ion species

- Divertor evolution during ELM-cycle
  - High recycling regime in the outer divertor connected to n_e recovery
    - ➢ Indication for change of particle transport

ASDEX Upgrade

Fusion@ÖAW

Backup

FRIEDRICH SCHIEDEL STIFTUNG FÜR ENERGIETECHNIK WIEN
F. M. Laggner is a fellow of the Friedrich Schiedel Foundation for Energy Technology

EUROfusion

This work has been carried out within the framework of the EUROfusion Consortium and has received funding from the Euratom research and training programme 2014-2018 under grant agreement No 633053. The views and opinions expressed herein do not necessarily reflect those of the European Commission.

Comparison to results from JOREK

- With diamagnetic rotation (tau_{IC}>0) high n are stabilized
  - Most unstable: 4 ≤ n ≤ 12 (here: n = 12)

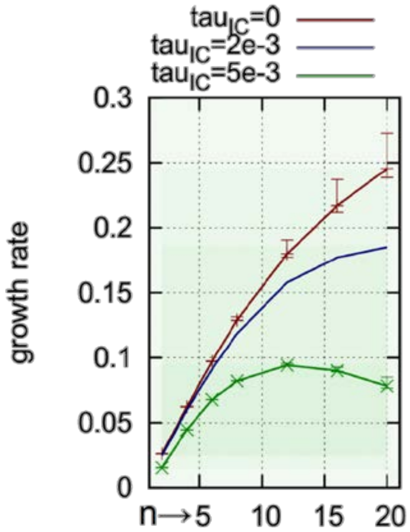

[F. Orain, A. Lessig et al., EPS 2016]

Comparison to results from JOREK

- With diamagnetic rotation (tau_{IC}>0) high n are stabilized
  - Most unstable: 4 ≤ n ≤ 12 (here: n = 12)

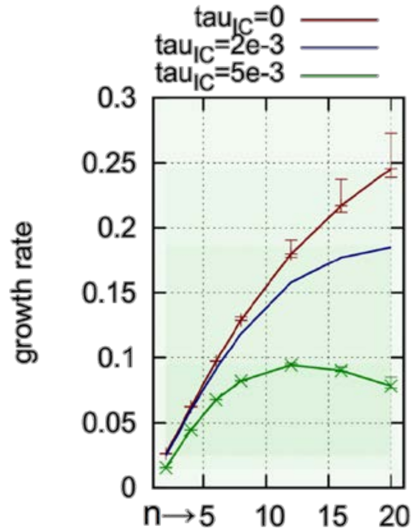

[F. Orain, A. Lessig et al., EPS 2016]

- Multi n simulation
  - •Medium n pre-ELM structures
  - •Non-linear coupling of medium n
    - ➢ Low n structures
    - [I. Krebs et al., PoP 2013]
  - •Saturation of modes
    - ➢ Clamping of ∇p ('soft limit')

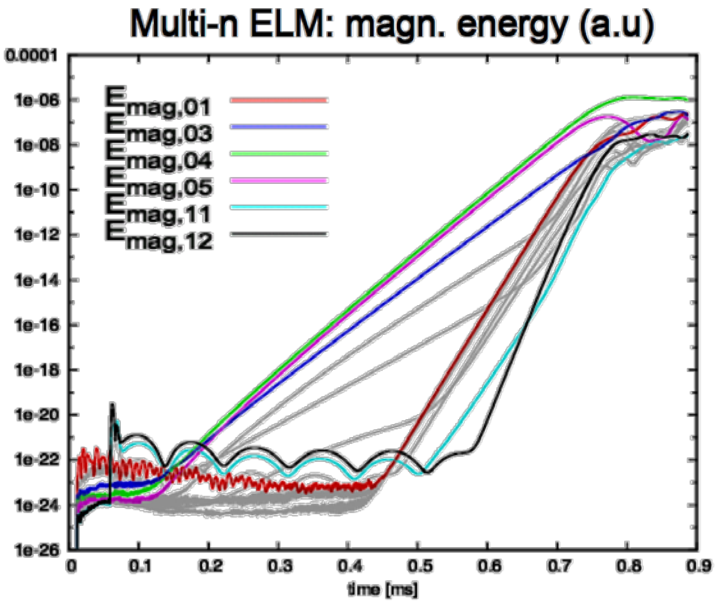

More frequent & larger ELMs in H

- f_{ELM} doubles from D to H
    - ELM frequency (f_{ELM})
- ΔW_{MHD} in H twice as large as in D
    - ELM energy loss (ΔW_{MHD})
- P_{ELM} 4 times higher in H than in D
    - Power loss by ELMs (P_{ELM})
- P_{net}-P_{ELM}-$P_{rad,sep}$ 1.8 times larger in H
    - Corrected heating power (P_{net})
    - Radiated power inside the separatrix ($P_{rad,sep}$)

D

f_{ELM} ~ 50 Hz

ΔW_{MHD} ~20 kJ

P_{net} ~3.8 MW

$P_{rad,sep}$ ~1.3 MW

H

f_{ELM} ~100 Hz

ΔW_{MHD} ~37 kJ

P_{net} ~7.3 MW

$P_{rad,sep}$ ~0.7 MW

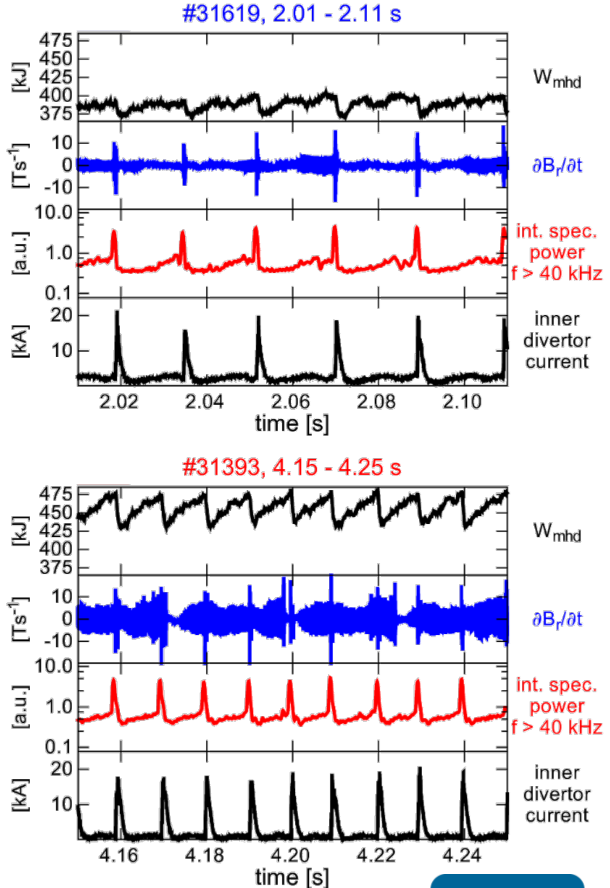

More frequent & larger ELMs in H

- f_{ELM} doubles from D to H
    - ELM frequency (f_{ELM})
- ΔW_{MHD} in H twice as large as in D
    - ELM energy loss (ΔW_{MHD})
- P_{ELM} 4 times higher in H than in D
    - Power loss by ELMs (P_{ELM})
- P_{net}-P_{ELM}-$P_{rad,sep}$ 1.8 times larger in H
    - Corrected heating power (P_{net})
    - Radiated power inside the separatrix ($P_{rad,sep}$)

➢ Larger power flux across the pedestal in H

D

f_{ELM} ~ 50 Hz

ΔW_{MHD} ~20 kJ

P_{net} ~3.8 MW

$P_{rad,sep}$ ~1.3 MW

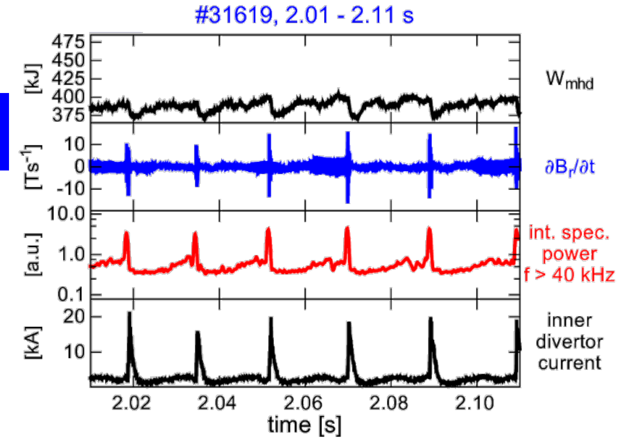

H

f_{ELM} ~100 Hz

ΔW_{MHD} ~37 kJ

P_{net} ~7.3 MW

$P_{rad,sep}$ ~0.7 MW

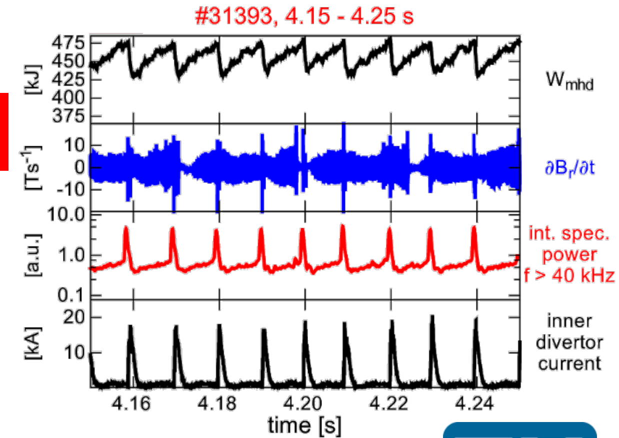

n_e pedestal evolution

- Δt_{n_e} longer in D in comparison to H
  - n_e pedestal recovery time (Δt_{n_e})

- Possible reasons
  - Gas fueling rate differs by a factor of ~10
  - Velocity of neutrals faster in H
    - Deeper neutral penetration
  - Increased outward particle transport from the core to the pedestal top

D

gas puff
$1.5\cdot10^{21}\ s^{-1}$

#31619, 2.00 - 2.11 s

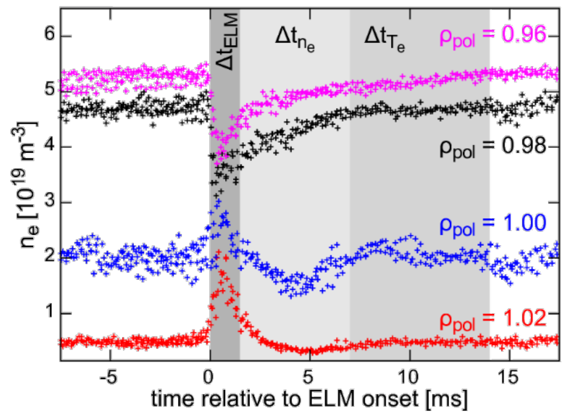

H

gas puff
$12\cdot10^{21}\ s^{-1}$

#31393, 4.10 - 4.35 s

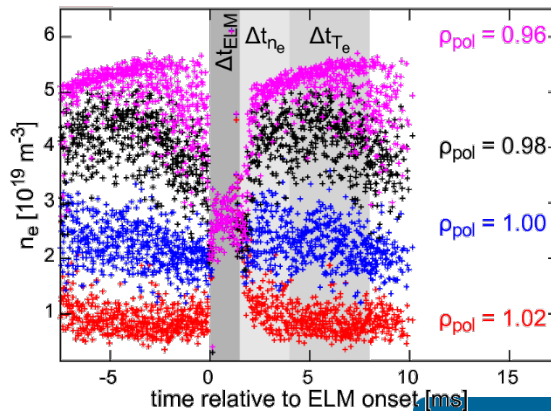

T_e pedestal evolution

- Δt_{T_e} faster in H
  - T_e pedestal recovery time (Δt_{T_e})
- Explanation
  - Larger heat flux to the pedestal in H
    - Higher P_{net}-$P_{rad,sep}$

D

P_{net}
~ 3.8 MW

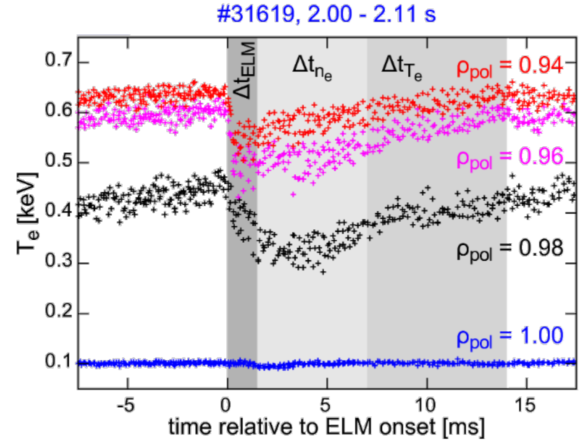

H

P_{net}
~ 7.3 MW

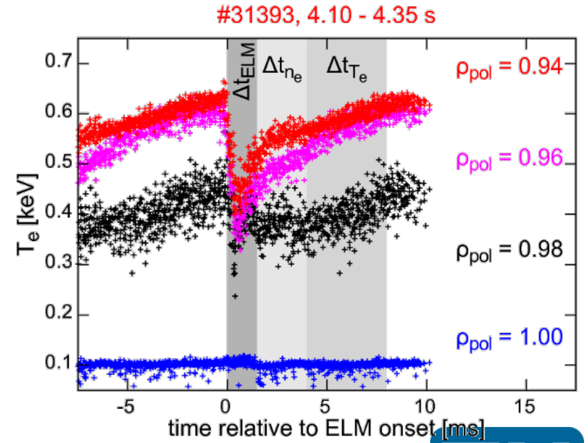

Magnetic signature

- $\partial B_r/\partial t$ measured at the LFS midplane
  - Radial magnetic fluctuations ($\partial B_r/\partial t$)
- Core modes
  - Frequency < 40 kHz
- Lower magnetic activity during Δt_{ne}
  - 40 kHz < frequency < 200 kHz
- After Δt_{Te} activity at high frequencies
  - Frequency > 200 kHz